N71- 35130

UTEC DO 71-155

SEMIANNUAL PROGRESS REPORT

NASA GRANT NO. NGL 45-003-029

M. L. Williams
Principal Investigator

K. L. DeVries
Co-Principal Investogator

University of Utah

13 August 1971

PREFACE

This project has developed along two separate but related lines. (1) The calculation and measurement of accumulation of damage in viscoelastic media and (2) the theoretical and experimental study of adhesive failure. Both studies have been progressing satisfactorily with particular success in the adhesive fracture area. Aspects of the other study have been reported in previous reports, and research now in progress will be reported at a later date.

We would like to briefly mention the interesting "spin off" from these efforts initially undertaken with NASA support. For example, the principles and methods developed under NASA have been used to develop a device and techniques to determine (under NIDR sponsorship) the quality of dental adhesives.

From the standpoint of continuum mechanics, there is an essential similarity between cohesive and adhesive failure. Continuum mechanics can therefore be used to analyze adhesive fracture including certain cases of interfacial debonding, by applying an extension of the Griffith cohesive fracture energy balance concept. Present researches permit a consideration of the influence of material behavior such as viscoelasticity and plasticity, and geometric parameters such as interlayer bond thickness. These advances and quantitative predictions of failure are reviewed with special reference to the characteristic adhesive fracture energy and its connection with the macro- and micro-constitution of the media. The determination of the adhesive fracture energy using a pressurized bubble or blister specimen is described in conjunction with experimental results from various materials using this test. The need for cooperation between continuum mechanics and chemistry is required as a matter of technological necessity in understanding the quality and efficiency of adhesive bonds. A method for associating the mechanical and chemical structure parameters, called the Interaction Matrix, is described as a device through which the required collaboration can be effectively channelled.

TABLE OF CONTENTS

INTRODUCTION

There appears to be a growing appreciation of the interdependence of mechanics and physical chemistry in the analysis and design of adhesive joints. The point of view of the present paper is from that of mechanics, with the objective of indicating how a wide variety of the characteristic features appearing in adhering systems can be analyzed with particular attention to predicting the debonding threshhold. Further, it is intended to focus attention upon those two material properties, namely deformation modulus and specific fracture energy, which are most directly associated with the chemistry and molecular structure of the material in order to encourage polymer and physical chemists to provide the analysts and materials engineers with the fundamental data required.

Since the early experimental work of de Bruyne[1] and the adhesive joint stress analysis proposed by Reissner and Goland,[2] there have been many contributions providing a more scientific background to assist the technological development. The review by Patrick[3] is typical of the state of the art, and in particular includes a discussion of the use of fracture mechanics ideas developed by Griffith for cohesive fracture of brittle materials. The adhesively bonded test specimen used by Ripling, et.al.[4] was one of the first to incorporate an energy criterion of failure as compared to the earlier ones using an allowable maximum stress or strain criterion.

Generally speaking, adhesively-bonded joints involve sharp corners and voids between adjacent different media which act as stress concentrators, particularly after a crack or imperfection arises at such a location. In a typical case consisting of two adherends and a third interlayer material as the bonding adhesive, there are several potential loci of failure, a cohesive failure in any of the three materials, or an adhesive failure at either of the two interfaces. The engineering problem is to determine the location of the weakest link and the magnitude of stress which is required to cause failure. The assessment proceeds from either of two points of view, depending upon whether or not inherent flaws or sharp corners are considered to be present.

In the first case the material is thought of as continuous, as in the normal tensile specimen, and a maximum tensile stress is obtained from the materials laboratory. Actually there is of course some reasonably uniform distribution of small voids present, whose size is related to the method of material fabrication. A simple example is a polymer which is mixed rapidly and contains finely dispersed air bubbles. Even with de-gassing, some distribution of flaws will exist on some dimensional scale. The average tensile strength therefore reflects their presence, and the dispersion of strength data about the norm describes the uniformity of the flaw distribution. Because most standard materials are made under reasonably controlled conditions, it is not surprising to find that some sort of consistent (average) stress or stress-functional criterion can be used to predict failure.

Under more complicated conditions, such as the multi-axial stressing of a turbine disk, it is customary to assume that the failure criterion is based on the octahedral shear stress (τ_{oct}) containing all three principal stresses (σ_i), and defined as

$$\tau_{oct} = K \sqrt{(\sigma_1 - \sigma_2)^2 + (\sigma_2 - \sigma_3)^2 + (\sigma_3 - \sigma_1)^2} \tag{1}$$

in which i = 1, 2, 3. Assuming the criterion applies, one predicts failure whenever this combination of principal stresses at any point in the part exceeds τ_{oct}. And how is τ_{oct} determined? If (1) is a <u>universal</u> failure criterion, it must also apply to the failure of a simple uniaxial tensile specimen having stresses $\sigma_1 = \sigma_{tens}$, and $\sigma_2 = \sigma_3 = 0$. Thus substituting into (1), find that

$$\tau_{oct} = K \sqrt{2\sigma_{tens}^2} \tag{2}$$

so that upon solving for the desired constant K and resubstituting into (1), one finds that failure is expected under a multi-axial principal stress combination whenever at some point in the body

$$\sqrt{(\sigma_1 - \sigma_2)^2 + (\sigma_2 - \sigma_3)^2 + (\sigma_3 - \sigma_1)^2} > \sqrt{2}\ \sigma_{tens} \tag{3}$$

or in the more general case, denoted as Region I (Figure 1), whenever

$$F(\sigma_1, \sigma_2, \sigma_3) > \sigma_{tens} \tag{4}$$

The octahedral stress criterion, which has been found by experience to work well for steel, is only one of several possibilities. Furthermore, the type of failure criterion, (4), is best used for smoothly varying stress fields with no exaggerated stress concentrations present and for materials having a uniform distribution of reasonably small micro-flaws.

The difficulty with many adhesive joints however is that they can possess very high stress concentration at corners or along bond lines, and usually contain substantially larger than average internal flaws, frequently as the result of absorbing water or poor wetting of the interfaces. In any event, the flaw distribution becomes denser and/or of larger size than the average size for which an average tensile strength would be appropriate. Thus the maximum permissible allowable stress is decreased. Griffith [5] provided the first estimate of the degradation as a function of the flaw size by considering the problem of a small, through, line crack in a thin sheet of brittle material. While theoretically the stress at the crack tips is (mathematically) infinite for an elastic body,[6] thus giving rise to an infinite local stress at even small applied loadings - a degree of concentration for which (4) is useless - Griffith avoided this problem by considering the strain energy in the sheet, which, as an integration of the stress, remained finite. He proposed that cohesive fracture would commence at a critical applied stress σ_{cr}, when the incremental loss of strain energy of deformation with increasing fracture area just exceeded the work required to create new fracture surface. Hence, in his case, with the strain energy of deformation due to $U = \pi a^2 \sigma_{cr}^2 / E$, the presence of the crack of length 2a being

$$\frac{\partial}{\partial a} \left[\pi a^2 \sigma_{cr}^2 / E \right] > \frac{\partial}{\partial a} \left[4 a \gamma_c \right]$$

from which the finite critical applied stress was determined.

$$\sigma_{cr} > \sqrt{\frac{2}{\pi} \frac{E \gamma_c}{a}} \tag{5}$$

3

in which E is Young's modulus, $\underline{a}$ the half-crack length, and γ_c the cohesive fracture energy density (in-lbs/in^2).

The combination of these two criteria, one flaw insensitive (Region I) and the other dependent upon flaw size (Region II) thus permits the designer to select a maximum allowable design stress providing he knows[±], or determines by tests in the laboratory on pre-cracked thin sheet tensile specimens with known crack size, the critical crack size, a*, shown in Figure 1. This critical size is deduced by the intersection of normal, nominally unflawed, tensile data (σ_{Fcr}) and initially pre-cracked sheet data which follows the Griffith curve (σ_{Gcr}). Once it is recognized that (4) and (5) are not competing failure criteria, but instead are complementary, it is possible to approach the design against failure in a more direct manner.

Turning now from cohesive to adhesive failure, it is merely necessary to establish that in principle and from the standpoint of a continuum mechanics analysis, cohesive and adhesive fracture are similar. Cohesive failure in any of the three materials of our earlier 3-layered bond example can thus be treated by (4) or (5). The new feature is how to treat an adhesive debonding at an interface. If there is no flaw at the interface, e.g., no surface roughness or air bubble, and no end to the joint, an unlikely situation, then in principle (4) can be applied on the basis of normal tensile testing of layered specimens - providing they do fail essentially at the bond line.

This situation would therefore correspond to a Region I type, average stress, adhesive failure. On the other hand, when voids and sharp corners are present - as is more customary - degradation of adhesive strength corresponding to a Region II type failure will occur and must be incorporated in the analysis.

As discussed more extensively in an earlier paper,[7] there is indeed a direct association between stress singularities, adhesion, and fracture. Consider for example the elastic analysis of a thin sheet in the neighborhood of a sharp geometric discontinuity such as a wedge point or crack tip, for which it is well known that a singularity in stress exists at the point of discontinuity and depends upon the local boundary conditions,

---

[±] The technically important problem of measuring the inherent flaw size in a part, preferably by some non-destructive test (NDT) method as ultrasonic wave reflection, X-ray, etc., will not be covered in this paper. Obviously if the inherent flaw size is unknown, a priori, the analyst does not know whether to choose Region I or Region II criteria.

loading, and properties of the material.[8-11] In the case of a central finite length crack in an infinite sheet subjected to tension, the classic Griffith problem gives a local stress variation which is proportional to the inverse square root of the distance from the crack tip.

Inasmuch as this (mathematically) infinite stress exists here for even the smallest loading, it appears that instantaneous fracture would occur and that a Region I criterion could not be used for predicting a finite stress which the sheet could withstand before fracture. The essential contribution of Griffith, however, was to develop the overall energy balance between the reduction in the deformational strain energy in the sheet and the energy required to create the new fracture surface. His result, (5), was the prediction of a finite applied tensile stress, σ_{cr}, needed to initiate fracture, namely, $\sigma_{cr} = \sqrt{2E\gamma_c/\pi a}$. It is apparent, therefore that the use of the integrated energy balance neatly circumvented the question of how infinite the infinite stress need become before fracture! It furthermore suggests the way in which other problems in stress analysis having stress singularities can be attacked in order to predict a finite stress at failure notwithstanding an infinite stress at the crack tip.

The character of elastic stress singularities to be expected for various geometric discontinuities was investigated by Williams[8,9] and later extended to the first analysis of the character of the stress singularities along the interface between dissimilar media.[12] In this case too, when a crack existed along the line of demarcation of the two materials, the stress singularity was likewise singular, although not necessarily solely of the $r^{-1/2}$ type*. It subsequently became attractive to inquire whether the same approach as Griffith used could be applied to predict the stress required to further separate or fracture the (adhesively bonded) interface between two different media, again notwithstanding the predicted existence of an infinite stress at the crack point for even small applied loads.

The phenomenological similarity in the two cases becomes clear. In the Griffith problem the finite length of the central crack 2a, lies, say,

---

* Actually in most cases a new characteristic oscillatory stress singularity arises although for a rigid-elastic incompressible interface it becomes identical to that for cohesive failure, i.e., $\sigma \sim r^{-1/2}$. (Reference 12.)

5

along the x axis, with the upper and lower half planes occupied by the same material; in the second problem, the materials above and below the x axis are different. For the purposes of discussion, we shall assume the material in the lower half plane to be infinitely rigid (e.g., glass) with respect to that in the upper half plane (e.g., rubber), and assume perfect adhesion over $|x| > a$. (Figure 2.) The stresses at the crack ends, $|x| = a$, are both singular. In the first case (Figure 2a) the Griffith critical stress is the classic example of cohesive fracture and well known; in the second (Figure 2b) the example of perfect adhesive failure is not.

Before looking into the second problem in more detail, it is pertinent to comment upon the distinction between the mechanics and chemistry viewpoints. As structured above, the mechanics approach is straightforward and consists of two parts: (1) conduct the stress analysis for an edge-bonded specimen having a central finite crack at the interface with a rigid boundary, and (2) express the incremental new surface energy generated as the crack extends. This latter part, however, requires interpretation.* In the cohesive fracture problem, with the same material on both sides of the extending crack, Griffith used $\Delta\Gamma = 4\gamma_c \Delta a$ as the incremental energy per unit thickness. The factor four arises because both ends of the crack are assumed to extend equally, and each end creates two new surfaces, one above and one below the crack. The specific energy γ_c has been subscripted to denote the value associated with cohesive failure. For adhesive failure, it would be appropriate, although not necessarily unique to write $\Delta\Gamma = 2\gamma_a \Delta a$ to denote that only two new free surfaces are formed in the elastic material. While this leaves open to surface chemists the question of any quantitative relation between γ_a and γ_c, as long as γ_a is a fundamental material constant, it can be used subsequently for predicting adhesive failure in a different geometric or loading configuration. Further discussion of this point will be delayed until later.

---

* It should be clear that a continuum mechanics analysis does not, of itself, differentiate between a cohesive or adhesive mechanism of failure. The distinction lies in the behavior implied by using a particular one of the respective energies in the formulas, namely γ_a (cohesive) or γ_a (adhesive). Furthermore there appears to be no direct association between the critical surface tension and the continuum mechanics analysis of the unstable infinitesimal deformation of a solid, although for special cases the critical surface stress to cause a spherical flaw to become unstable has been deduced by Williams and Schapery.[13,14]

We are able to conclude therefore, phenomenologically, that there is
an equivalent Griffith-type adhesive fracture problem for which the continuum
mechanics analysis is essentially the same as for cohesive fracture. The
difference lies in the interpretation attached to the specific fracture
energy, γ, and, in some cases, possible additional material modulus
properties on either side of the crack. The analogy is complete and results
similar to (5) can be obtained, except that the *adhesive* fracture energy
must be used in the criticality condition, i.e., (Figure 2b)

$$\sigma_{cr} = \sqrt{\frac{2}{\pi} \frac{E\gamma_a}{a}} \tag{6}$$

to predict adhesive fracture between a rigid-incompressible material com-
bination. Hence with this connection formally established, the entire body
of analytical knowledge in cohesive fracture mechanics can be transferred
to analyze adhesive debonding.

The following examples will serve to illustrate the point on both an
approximate and exact basis.

ANALYTICAL DETERMINATION OF ADHESIVE FRACTURE ENERGY - ELASTIC

The Basic Concept

The simplest illustration of the concept involved borrows from the
Obreimoff[15] proposition for determining cohesive fracture energy by using
a split cantilever beam. (Figure 3) The strain energy stored in the top
linear elastic beam, assumed clamped at the end of the split, is one half
of the work done by the applied force (F) acting through the equilibrium
displacement.

$$U = \frac{1}{2} \cdot F \cdot \frac{FL^3}{3EI} \tag{7}$$

in which $I = b(2t)^3/12$ is the moment of inertia. Also the incremental
increase in the new area, counting only that associated with the top beam
in order to be consistent with (7), is $\partial\Gamma = \gamma_c \partial(L \cdot b)$. Thus, equating the
two, one finds

$$\gamma_c = \frac{\partial \Gamma}{\partial (L \ b)} = \frac{\partial U}{\partial (L \ b)} = \frac{F^2 L^2}{2bEI} = \frac{6F^2 L^2}{Eb^2 (2t)^3} \qquad (8)$$

or in terms of the maximum outer fiber stress σ_0 developed at the bonded end

$$\sigma_0 = \sqrt{3\gamma_c E/t} \qquad (8a)$$

from which γ_c can be deduced from the measurable quantities in (8) at the instant of fracture.

If now the geometry of Figure 3 is changed such that the top beam is bonded to a rigid substrate instead of to its mirror image, a little reflection indicates that within the approximation of elementary beam theory the analysis is identical to (8) except that the quantity which will be deduced is γ_a, the *adhesive* fracture energy required to separate the beam from its attachment.

Centrally Unbonded Thick Plate of Finite Thickness. (Figure 4a)

Another fairly simple example, and one which permits a reasonable degree of generality for illustrating several other characteristics later, is an elastic strip plate of width 2a, infinite length, and thickness, h. Depending upon the thickness of the plate, it may be analyzed as one containing predominantly bending energy ("thick plate"), stretching energy with little bending energy ("membrane"), or a combination of the two ("thin plate"). The elementary calculation[16] paralleling (8) above would be for a thick plate in which case the classical strip plate equation for a uniform pressure loading is

$$D \frac{d^4 w}{dx^4} = p \qquad (9)$$

from which, for clamped ends at $|x| = a$,

$$w(x) = \frac{p}{24D} [a^2 - x^2]^2 \qquad (10)$$

Again utilizing Clapeyron's Theorem[17]

$$U = \int_{-a}^{a} \frac{p}{2} \left[\frac{p}{24D} (a^2 - x^2)^2 \right] dx = \frac{p^2 a^5}{45D} \qquad (11)$$

8

and assuming debonding at both ends such that for a unit length of the strip, one finds that

$$\gamma_a = \frac{\partial U}{\partial (2a)} = \frac{p^2 a^4}{18D} = \left[\frac{2(1-\nu^2)}{3}\left(\frac{a}{h}\right)^3\right]\frac{p_{cr}^2 a}{E} \qquad (12)$$

The above simple illustrations incorporate several approximations which do not exactly reflect the actual plate behavior, namely: (a) plane sections do not remain plane especially near the end of the crack; (b) there will be some stress and some strain energy stored in that part of the beam past the assumed fixed end at L; (c) there will be (mathematically) infinite stresses at the point of the crack; (d) plastic flow probably occurs at the crack tip; and (e) the fracture criticality condition is only a necessary one. Nevertheless, information useful in design is obtained, mainly because the values of γ_c and γ_a so obtained are used in analyzing applications incorporating the same approximations.

Centrally Unbonded Block of Infinite Extent. (Figure 4b)

It is not necessary however, as far as continuum mechanics stress analysis is concerned and the problem demands, to accept all of these confining assumptions. If the thickness of the plate of the previous example increases, it finally becomes so thick that simple plate theory is no longer applicable. In the limit therefore, one considers a semi-infinite half space which is unbonded over a width 2a and infinite length. Unfortunately this analysis is not as simple to reproduce, but suffice it to say that a biharmonic boundary value problem in elasticity is formulated from which the stresses, strains, and strain energy density in the medium can be calculated.[18] The singular stresses are automatically incorporated in the analysis, and no plane section simplifying assumptions are needed. Plasticity so far however has not been included. After integrating the strain energy of deformation over the volume, and equating its change with respect to increased debond area to the adhesive fracture energy, one finds that

$$p_{cr} = \sqrt{\frac{8}{3\pi}\frac{E\gamma_a}{a}} \qquad : \quad \nu = 1/2 \qquad (13)$$

or in terms of γ_a,

$$\gamma_a = \frac{3\pi}{8}\frac{p_{cr}^2 a}{E} = \frac{3\pi}{8}\cdot\frac{p_{cr}^2}{E}\cdot a \qquad (14)$$

9

which can be compared with (12).

Centrally Unbonded Thin Plate of Finite Thickness.

Another related geometry can also be easily dealt with. When the
plate thickness becomes rather small, the stretching energy due to in-
plane stresses increases compared to the bending energy. Indeed, in
the limited case of a very thin plate or membrane, the bending energy is
vanishingly small compared to the energy of stretching. A rubber balloon
falls into this category and its non-linear increase in size with internal
pressure is a matter of common experience. In this case, one finds it
necessary to consider both the stretching displacement, $u(x)$, as well as
the normal bending deflection, $w(x)$. Two differential equations are
involved, but the solution for an infinite length strip unbonded over a
length 2a, and clamped at both ends is available;[19,20] actually for both
a pressure and temperature loading. The latter solution may be expected to
be of some value in conjunction with estimating debonding due to the curing
stresses after polymerization.

The governing differential equations are (for constant material pro-
perties, plate thickness, pressure, and temperature drop, ΔT)

$$D \cdot \frac{d^4 w}{dx^4} - N \frac{d^2 w}{dx^2} = p. \tag{15}$$

$$\frac{du}{dx} + \frac{1}{2}\left(\frac{dw}{dx}\right)^2 - (1 + \nu)\, \alpha \Delta T = \frac{(1 - \nu^2)\, N}{Eh} \tag{16}$$

along with boundary conditions, assuming clamped ends, of

$$u(\pm a) = w(\pm a) = dw(\pm a)/dx = 0 \tag{17}$$

the solution scheme is to solve (15) for $w(x)$, then insert it into (16) to
integrate for $u(x)$. The constant in-plane stress, $N = \sigma_s \cdot h$, is determined as
the boundary conditions (17) are applied. For our purposes, the two phy-
sically interesting cases are (i) when the bending rigidity is vanishingly
small, thus corresponding more to a thin, very flexible, film bonded to
the substrate, and (ii) when the bending and stretching energies are

10

comparable, as might be the case for certain dimensions of a paint blister or an automobile metal part.

From these basic formulas, it is straight forward to calculate the energy balance. The input work, I, must be balanced by the strain energy of deformation, U, stored within the body and the work to create new fracture surface Γ. (Kinetic effects are neglected.) Hence one finds, for uniform pressure and constant temperature change, ΔT,

$$I = \int_{-a}^{a} p \, w \, (x) \, dx \tag{18}$$

$$U = \int_{-a}^{a} \left\{ \frac{Eh}{2(1 - \nu^2)} \left[\left(\frac{dv}{dx}\right) + \frac{1}{2}\left(\frac{dw}{dx}\right)^2 \right]^2 - \frac{E \, h \, \alpha \, \Delta \, T}{1 - \nu} \left[\frac{dv}{dx} \right. \right.$$
$$\left. \left. + \frac{1}{2}\left(\frac{dw}{dx}\right)^2 \right] \right\} dx + \int_{-a}^{a} \frac{D}{2} \left(\frac{d^2w}{dx^2}\right)^2 dx \tag{19}$$

in which the first and second terms of U represent stretching and bending contributions respectively, and

$$\Gamma = \int_{-a}^{a} \gamma \, dx \tag{20}$$

Williams[19,20] has given the general solutions for this problem, actually including varying pressure, temperature, and material properties, as well as for both clamped and simply supported plate bondary conditions. (Note for example that if the cover sheet shrunk less than the substrate, a buckling condition in the sheet could arise!) From these more general solutions and graphs of the results, it is a sufficient illustration for our present purpose to extract only one of the simpler results to show the extent of more sophisticated analysis which is available if desired or necessary.

Membrane strip. In this case when bending energy can be neglected, the basic equations (15) and (16) reduce to

11

$$-N \left(d^2w/dx^2 \right) = p \qquad (21)$$

$$\frac{du}{dx} + \frac{1}{2}\left(\frac{dw}{dx}\right)^2 - (1 + \nu)\alpha\Delta T = \frac{(1 - \nu^2)N}{Eh} \equiv \Sigma_s \qquad (22)$$

with boundary conditions

$$w(\pm a) = u(\pm a) = 0 \qquad (23)$$

Upon integrating (21)

$$w(x) = w_0 \left[1 - (x^2/a^2)\right] \quad ; \quad w_0 = pa^2/2N \qquad (24)$$

and insertion into (22), one finds

$$u(x) = \left[(1 + \nu)\alpha\Delta T + \frac{1 - \nu^2}{2} \frac{pa^2}{Ehw_0}\right] x - \frac{2}{3} \frac{w_0^2 x^3}{a^4} \qquad (25)$$

whereupon after applying the boundary conditions, (23), the (constant) stress in the membrane becomes*

$$\sigma_s \equiv N/h = \frac{pa^2}{2w_0 h} = \frac{2E}{3(1 - \nu^2)} \left(\frac{h}{a}\right)^2 \left[\left(\frac{w_0}{h}\right)^2 - \frac{3}{2}(1 + \nu)\alpha\Delta T\left(\frac{a}{h}\right)^2\right] \qquad (26)$$

It is now straightforward to compute the energies (18) - (20) as

$$I = \int_{-a}^{a} pw_0 \left[1 - (x^2/a^2)\right] dx = (4/3) pw_0 a$$

$$= \frac{8}{3}\left(\frac{w_0}{a}\right)^2 \left[\frac{2}{3}\left(\frac{w_0}{a}\right)^2 - (1 + \nu)\alpha\Delta T\right] \frac{Eh}{1 - \nu^2} \qquad (27)$$

---

* This expression denoting equilibrium positions for maximum membrane deflection for various combinations of pressure and temperature can be cast into the following form and plotted (see Reference 19)

$$\left[\left(\frac{w_0}{h}\right)^2 - \frac{3}{2}(1 + \nu)\alpha\Delta T \left(\frac{a}{h}\right)^2\right] \frac{w_0}{h} = \frac{3(1 - \nu^2)}{4} \frac{pa^4}{Eh^4} \qquad (26a)$$

12

$$U = \int_{-a}^{a} \left\{ \frac{Eh}{2(1-\nu^2)} \left[\frac{(1-\nu^2)N}{Eh} + (1+\nu)\alpha\Delta T \right]^2 - \frac{Eh\alpha\Delta T}{1-\nu} \left[\frac{(1-\nu^2)N}{Eh} + (1+\nu)\alpha\Delta T \right] \right\} dx$$

$$= \frac{4}{3} \left(\frac{w_0}{a} \right)^2 \left[\frac{1}{3} \left(\frac{w_0}{a} \right)^2 - (1+\nu)\alpha\Delta T \right] \frac{Eh}{1-\nu^2} \tag{28}$$

$$\Gamma = 2a\gamma_a \tag{29}$$

From these expressions one finds after a bit of algebraic manipulation, that

$$I-U = \frac{4}{3} \frac{Eha}{1-\nu^2} \left(\frac{w_0}{a} \right)^2 \left[\left(\frac{w_0}{a} \right)^2 - (1+\nu)\alpha\Delta T \right] \tag{30}$$

Upon computing for the criticality condition at constant pressure

$$\partial\Gamma/\partial a = 2\gamma_a = \partial(I - U)/\partial a \tag{31}$$

in which from (26) one finds

$$\frac{\partial w_0}{\partial a} \Big|_p = \frac{[(1 - \nu^2)pa/Eh] + (w_0/a)(1 + \nu)\alpha\Delta T}{(w_0/a)^2 - (1 + \nu)\alpha\Delta T/2} \tag{32}$$

The result is

$$\gamma_a = \frac{4Eh}{3(1 - \nu^2)} \left(\frac{h}{a} \right)^4 \left[\frac{7}{6} \left(\frac{w_0}{h} \right)^2 - \frac{3}{2} (1 + \nu)\alpha\Delta T \left(\frac{a}{h} \right)^2 \right] \left(\frac{w_0}{h} \right)^2 \tag{33}$$

where in terms of ready comparison with the thick plate results (w_0/h) must be eliminated from (33) using (26). In the simple case, for example, of no heating $\Delta T = 0$, and

$$\frac{\gamma_a/a}{E} \Big|_{\Delta T=0} = \frac{7}{6} \sqrt[3]{\frac{3(1 - \nu^2)}{4} \left(\frac{a}{h} \right) \left(\frac{p_{cr}}{E} \right)^4} \tag{34}$$

or in terms of the critical pressure for a known adhesive fracture energy

$$\frac{P_{cr}}{E} = \sqrt[4]{\frac{288}{344(1 - \nu^2)}} \left(\frac{h}{a}\right)^{1/4} \left(\frac{\gamma_a/a}{E}\right)^{3/4} \qquad ; \text{ membrane} \qquad (35)$$

which values are of interest to compare to the previously derived ones

$$\frac{P_{cr}}{E} = \sqrt[2]{\frac{3}{2(1 - \nu^2)}} \left(\frac{h}{a}\right)^{3/2} \left(\frac{\gamma_a/a}{E}\right)^{1/2} \qquad ; \text{ thick plate} \qquad (36)$$

$$\frac{P_{cr}}{E} = \sqrt{\frac{8}{3\pi}} \left(\frac{\gamma_a/a}{E}\right)^{1/2} \qquad ; \text{ infinite block} \quad (37)$$

As all the numerical constants are of order unity, it is interesting to note that for the same materials the critical stress predicted for thinner membranes is substantially above that predicted using plate theory. The specific transition from the thick plate through the thin plate regime to the membrane can be deduced if desired using the appropriate thin plate expressions from Reference 19.

Thermal Debonding of a Membrane. Another simple calculation can also be made as an outgrowth of the foregoing analysis, and illustrates the type of estimates which can be made for blisters which debond from surfaces, as in paint, when subjected to too much heat. While the basic solution for an arbitrarily variable temperature distribution through a thin plate is given in Reference 20, it is particularly easy to see the nature of the result from the criticality condition (33), in which the value of w_o/h to be inserted is taken from the possible equilibrium conditions of the strip in (26a). For example, if there is no imposed pressure, and the temperature is uniformly distributed through the, in this case, membrane, (26) gives

$$w_o/a \Big|_T = \left[(3/2)(1 + \nu)\alpha\Delta T\right]^{1/2} \qquad (38)$$

thus in (33) ΔT_{cr} to cause unbonding is

$$\gamma_a = \frac{4}{3} \frac{Eh}{1 - \nu^2} \left[\frac{7}{6}\left(\frac{w_o}{a}\right)^2_T - \frac{3}{2}(1 + \nu)\alpha\Delta T\right]\left(\frac{w_o}{a}\right)^2_T = \frac{Eh}{2} \frac{1 + \nu}{1 - \nu}(\alpha\Delta T)^2$$

14

or

$$\Delta T_{cr} = \sqrt{\frac{2(1 - \nu)}{1 + \nu} \frac{\gamma_a/h}{E\alpha}} \tag{39}$$

which should give a reasonably good estimate for very thin polymer films. For thicker or metallic films for which the product $E\alpha$ is characteristically larger, the more complete analysis[19] must be used.

In any event, the point of this section is to show that continuum mechanics can in principle be developed to treat the rather complicated problem of adhesive debonding of a heated or, what is the same thing, cure shrunk bond. The only real question is the practical one of required accuracy for time invested within the economical necessity.

Localized Modulus Variation near the Interface

It frequently happens that there are localized changes in the material properties of two different materials when they are placed in contact. On the one hand they can be due to chemical interaction, or frequently more mechanical as when a liquid polymer is cast and cured against a fixed surface. In this latter case, the random growth of the polymer chains is inhibited as they approach the fixed boundary and tend to bend and lie parallel to its surface. The net result is a localized boundary layer or "skin effect", which is expected to produce a different result than if the, say, material modulus was uniform directly up to the interface.

Again we find there are two ways of approaching this problem from the point of view of continuum mechanics. First of all, it makes little difference in principle to a stress analysis as to whether the material properties are isotropic, anistotropic, or inhomogeneous. In practice however, it is usually more desirable to obtain a qualitatively correct answer and improve it to the degree required. This philosophy is pertinent here, and the problem could be formulated as one of two dissimilar orthotropic materials bonded along the abscissae $x > 0$ and free along $x < 0$. Actually this was done several years ago in one case in conjunction with analyzing the characteristic stresses which might arise in the vicinity of a geophysical fault between two strata[12]. In that case however, the material properties above and below the fault were assumed individually and separately isotropic and homogeneous. An analytical extension of this problem based upon

our earlier work[10,11] and now being completed, assumes that there are orthotropic properties in the media, essentially such that the Young's modulus $E = E(y)$, to account for a harder or softer material near the interface than in the interior.

A more direct way of exhibiting the general effect however is to use the simpler case of a split beam, in order to show again that this variation can be treated - and improved upon in accuracy as the circumstances warrent. Consider, therefore, the plate strip shown in Figure 5, where the origin of the axis of y is at the bottom of the thickness, h. After assuming plane sections remain plane under bending, only two conditions are required. First, by assumption, the sum of the x-forces integrated with respect to y, Nx, are zero, and the moment of the internal stresses must equal the external moment. Hence if N is the force per unit width of the strip in the z-direction

$$N_x(x) = \int_0^h \sigma_x(y)dy = \int_0^h \frac{E(y)}{1 - \nu^2} E_x(y) \, dy \tag{40}$$

whereas the moment per unit strip width is

$$M = \int_0^h \sigma_x(y) \, y \, dy = \int_0^h \frac{E(y)}{1 - \nu^2} E_x(y) \, y \, dy \tag{41}$$

where the factor $1 - \nu^2$ arises because an infinite stress p width has been assumed. Now assuming that plane sections remain plane,

$$\varepsilon_x(y) = (y - \bar{h}) \frac{\partial^2 w(x)}{\partial x^2} \tag{42}$$

where $y = \bar{h}$ is the zero extensional fiber, and selecting a representative modulus variation which can represent any rather arbitrary localized skin effect or boundary layer, namely

$$E = E_0 + E_1 \exp(-\lambda y/h) \tag{43}$$

one can substitute (42) and (43) into (40) and (41), and first find $\bar{h}$ by the condition that $N_x = 0$, viz.

$$\frac{\bar{h}}{h} = \frac{\frac{1}{2} - \frac{E_1}{E_0} \frac{1}{\lambda} \left[e^{-\lambda}(1 + \frac{1}{\lambda}) - \frac{1}{\lambda} \right]}{1 - \frac{E_1}{E_0} \frac{1}{\lambda} \left[e^{-\lambda} - 1 \right]} \cdot \tag{44}$$

where is may be noted that $\bar{h}/h = 1/2$ as it should if E_1 is zero, i.e., no anisotropic modulus.

Secondly, the moment relation from (41) becomes

$$M = \frac{d^2 w}{dx^2} D = \frac{d^2 w}{dx^2} \frac{E_0 h^3}{12(1 - \nu^2)} g\left(\lambda, \bar{h}, \frac{E_1}{E_0}\right) \tag{45}$$

where

$$g\left(\lambda, \bar{h}, \frac{E_1}{E_0}\right) = 12 \left[\frac{1}{3} - \frac{1}{2} \frac{\bar{h}}{h} \right] - 12 \frac{E_1}{E_0} \left[\left(\frac{1}{\lambda} + \frac{2}{\lambda^2} + \frac{2}{\lambda^3} \right) e^{-\lambda} - \frac{2}{\lambda^3} \right.$$
$$\left. - \left(\frac{1}{\lambda} + \frac{1}{\lambda^2} \right) \frac{\bar{h}}{h} e^{-\lambda} + \frac{1}{\lambda^2} \frac{\bar{h}}{h} \right] \tag{46}$$

Note that any further analysis for this plate strip can proceed as before except that now $D = D\left[\lambda, \bar{h}(\lambda)\right] = D(\lambda)$.

In most cases of adhesive joints the chemical or mechanical effect dies away very rapidly such that the decay constant, λ, in (43) is quite large, typically of the order of 10-20 and $E_1/E_0 < 1$. Under these conditions (44) and (46) may be further approximated by

$$\left. \frac{\bar{h}}{h} \right|_{\lambda \gg 1} \sim \frac{1}{2} \left[1 - \frac{E_1}{E_0} \cdot \frac{1}{\lambda} \right] \tag{44a}$$

$$\left. g(\lambda) \right|_{\lambda \gg 1} \sim 1 + \frac{3}{\lambda} \frac{E_1}{E_0} \tag{46a}$$

If, therefore, we consider the centrally unbonded pressurized strip, (12), the first approximation accounting for a skin effect would be

$$\gamma_a = \frac{p^2 a^4}{18 D} = \frac{p^2 a^4}{18 D_0} \left[1 - \frac{3}{\lambda} \frac{E_1}{E_0} + \cdots \right] \tag{47}$$

There are two questions to be answered here however. First, whether the formula is being used to measure γ_a from (47), or second, whether γ_a

17

is known from, say, an independent measurement and the effect of a change in the surface modulus, $E_s = E_0 + E_1$, upon bond strength is being examined. In the latter form, with γ_a fixed by the interface conditions, the inversion of (12) to

$$P_{cr} = \sqrt{\frac{3}{2} \frac{(E_0 + E_1)\, \gamma_a/a}{(1 - \nu^2)} \left(\frac{h}{a}\right)^3} \left\{ \frac{1 + \dfrac{3}{2\lambda} \dfrac{E_1}{E_0} + \cdots}{1 + \dfrac{E_1}{E_0}} \right\}^{1/2} \qquad (48)$$

The correction factor in brackets is plotted in Figure 5 and shows for example, that if the stiffness in the interior is substantially less than the interface stiffness, measured by the decay constant λ, the bond strength will drop off according to (48). Contrarily, if any softening lies at the interface, with complete (harder) cure in the interior, the bond strength will increase.

To reiterate however the first point, if the test is being used to deduce γ_a, and the bulk property away from the interface, i.e., E_0, is being used in the formulas, then only an apparent value of γ_a will be calculated, within the factor $g(\lambda_1, E_1/E_0)$.

The Effect of an Intermediate Adhesive Interlayer.

While in some cases it is sufficient to consider only a bimaterial system, such as a plate or block cast onto a substrate, it more frequently happens that two pre-formed materials are bonded together with a third, adhesive, material. There has been frequent discussion on the relative merits of this interlayer material, such as it should have a high modulus, or be very thin. It is possible to analyze a model of such a multi-layer bonded joint, and the one chosen for illustrative purposes consists of a centrally unbonded elastic strip plate bonded to a rigid substrate by an elastic adhesive of different material properties (E', ν') and thickness (h')[21]. The same elementary plate theory approach can be used in which it is assumed the adhesive interlayer behaves as a common Winkler foundation of modulus, k. It proves possible to estimate rather easily the effect of the interlayer, as shown in Figure 6, for a long, centrally debonded, sheet[21] or for a circular[22] blister specimen. (The cross-section shown in Figure 6 would be the same in either case, although in

practice the centrally unbonded strip geometry is of course more diffi-
cult to test because it is not easy to seal the ends when the specimen is
pressurized).

For illustrative purposes however, because the formulas are simpler,
consider the centrally bonded strip as a clamped beam (Figure 6). The
solution of the field equation for $|x| < a$

$$D(d^4w/dx^4) = p \tag{49}$$

is

$$Dw(x) = C_0 + (C_2 x^2/2) + (px^4/24) \tag{50}$$

For the external region, $|x| < a$, one assumes an elastic foundation with
modulus k, giving

$$D(d^4w/dx^4) + k w = 0 \tag{51}$$

with solution

$$w(x) = (C_3 \cos \lambda x + C_4 \sin \lambda x) \exp(-\lambda x) \tag{52}$$

in which the definitions

$$D \equiv Eh^3/[12(1 - \nu^2)] \; ; \quad k \equiv 4D\lambda^4 \; ; \quad \mu \equiv a\lambda \tag{53}$$

have been used. The solution as obtained earlier[21] gives

$$C_0 = pa^4 \left[\frac{1}{24} + \frac{2\mu^3 + 5\mu^2 + 6\mu + 3}{12\mu^3 (1 + \mu)} \right] \tag{54}$$

$$C_2 = pa^2 \left[\frac{1}{6} + \frac{2\mu + 3}{6\mu (1 + \mu)} \right] \tag{55}$$

$$C_3 = \frac{pa^4}{D \exp(-\lambda a)} \left[\frac{(2\mu^2 + 6\mu + 3) \cos \mu + (2\mu^2 - 3) \sin \mu}{12\mu^3 (1 + \mu)} \right] \tag{56}$$

$$C_4 = \frac{pa^4}{D \exp(-\lambda a)} \left[\frac{(2\mu^2 + 6\mu + 3) \sin \mu - (2\mu^2 - 3) \cos \mu}{12\mu^3 (1 + \mu)} \right]_{(57)}$$

Upon calculating the strain energy of deformation, and assuming uniform pressure

$$U = \frac{1}{2} \int_{-a}^{a} pw \, dx = \frac{pa^5}{45D} \left[1 + \frac{5}{4} \frac{4\mu^3 + 12\mu^2 + 18\mu + 9}{\mu^3 (1 + \mu)} \right] \quad (58)$$

Then upon equating $\partial U / \partial a$ (for a unit length of the plate strip) to $\partial \Gamma / \partial a = 2\gamma_a$, where the factor $\underline{2}$ accounts for simultaneous debonding at both ends, one finds the critical pressure at incipient debonding as*

$$p_{cr}^2 \cong \frac{\frac{3}{2(1 - \nu^2)} \left(\frac{h}{a}\right)^3 \frac{E\gamma_a}{a}}{1 + \frac{16\mu^4 + 56\mu^3 + 84\mu^2 + 63\mu + 18}{4\mu^3 (1 + \mu)^2}} = \frac{\frac{3 (h/a)^3}{2(1 - \nu^2)} \frac{E\gamma_a}{a}}{1 + \phi(\mu)} \quad (59)$$

where it may be noted that for zero thickness bond layers, i.e., $k \sim h' \to 0$, the zero interlayer solution corresponding for example to polymer being cast directly onto the substrate, is recovered.

Indeed for many practical geometrical combinations, μ tends to be rather large, in which case (20) can be approximated by

$$[1 + \phi(\mu)]^{-1} = 1 - 4\sqrt[4]{\frac{1}{3} \left(\frac{h}{a}\right)^3 \frac{E}{ka}} + \ldots = 1 - 4 \frac{h}{a} \sqrt[4]{\frac{(1+\nu')(1-2\nu')}{3(1-\nu')(1-\nu^2)} \frac{E/h}{E'/h'}} + \ldots \quad (60)$$

in which the primed quantities refer to the interlayer. For this situation, for example, the critical pressure to cause failure decreases with either a stiffer interlayer modulus or a reduced interlayer thickness.

$$p_{cr} \cong \sqrt{\frac{3(h/a)^3}{2(1 - \nu^2)} \frac{E\gamma_a}{a}} \left[1 - 2 \frac{h}{a} \sqrt[4]{\frac{(1 + \nu')(1 - 2\nu')}{3(1 - \nu')(1 - \nu^2)} \frac{E/h}{E'/h'}} \right]$$

---

* In reference (21), equation (14) is improperly described as the result for a plate strip. It is actually that for a beam strip of unit width. The plate strip solution is derived from the beam strip by replacing E by $E/(1 - \nu^2)$, which latter value for an incompressible material is $4E/3$. Replacing E by $E/(1 - \nu^2)$ in that equation (14) gives the result in (59) to follow.

$$\cong p_{cr}^{(0)} \left[1 - C \left(\frac{h'}{E'} \right)^{\frac{1}{4}} + \cdots \right] \tag{61}$$

It should also be noted that it is the <u>ratio</u> of h'/E' that is the major controlling parameter, not the modulus or thickness separately. This point probably has more general practical implications.

<u>Interlayer Between Two Different Media</u>. The previous case can be further extended to include the situation in which the substrate is not rigid. Providing only that the Winkler type foundation hypothesis used in (51) is still valid, i.e., the adhesive reacting force is essentially proportional to the deflection, f = kw, thus neglecting shear stress in the adhesive interlayer, one can allow for an elastic interlayer between two sheets of different material properties and thickness (Figure 7).

Denoting the upper cover sheet by unprimed quantities, the interlayer properties by primes, and the lower sheet quantities by bars, one can deduce the strain energy in the combined system. There are three possible loci of failure. First at the interface between the top sheet and interlayer (p_{cr}), second, at the interface between the bottom sheet and interlayer $(\bar{p}_{cr})$, and third, a cohesive failure in the adhesive itself. The results can be summarized as follows:

$$p_{cr}^2 = \frac{\dfrac{3(h/a)^3}{2(1-\nu^2)} \dfrac{E\gamma_a}{a}}{1 + \phi(\mu)} \cdot \frac{1}{1 + \dfrac{1 + \phi(\bar{\mu})}{1 + \phi(\mu)} \cdot \dfrac{\bar{D}}{D}} \tag{62a}$$

$$\bar{p}_{cr}^2 = \frac{\dfrac{3}{2} \dfrac{(\bar{h}/a)^3}{(1-\nu^2)} \dfrac{\bar{E\gamma}_a}{a}}{1 + \phi(\bar{\mu})} \cdot \frac{1}{1 + \dfrac{1 + \phi(\mu)}{1 + \phi(\bar{\mu})} \cdot \dfrac{D}{\bar{D}}} \tag{62b}$$

The lower of (62) and (63), which depends not only upon the appropriate adhesive fracture energies γ_a or $\bar{\gamma}_a$ but also upon the other material properties and thickness, thus give the criticality estimate and location.

It could also happen that the interfacial strengths are both sufficiently high such that cohesive failure may arise in the interlayer itself. An approximation to the stress field for this pressurized blister geometry gives the maximum tensile stress at the edge of the interlayer, x = a, as

$$f(a) = p \left\{ \frac{\mu}{3(1 + \mu)} [2\mu^2 + 6\mu + 3] + \frac{\bar{\mu}}{3(1 + \bar{\mu})} [2\bar{\mu}^2 + 6\bar{\mu} + 3] \right\} \tag{63}$$

which magnitude may also be compared to those in (62). If the free edge of the interlayer (Figure 7) has a crack in it of depth c, then the magnitude of (63) will be further concentrated. Using again fracture theory in the form of the critical (assumed average) uniform tensile stress $\bar{f}(a)$ to cause cohesive fracture in an edge notched tensile strip of incompressible material subjected to plane strain, one finds

$$\bar{f}(a)\Big|_{cr} \simeq \sqrt{\frac{2}{3} \frac{E' \gamma_c'}{c}} \tag{64}$$

in which γ_c' refers to the cohesive fracture energy of the interlayer material.

These latter results, (62-64), have not been confirmed by experiment. At the present time therefore, they should be viewed as illustrations of the manner in which an adhesively bonded joint might be simply analyzed, providing other independent tests, e.g., rigid pressurized blister, have yielded design data for γ_a, $\bar{\gamma}_a$, and γ_c'.

APPLICATIONS TO NON-ELASTIC FAILURE

There are two other adhesive debonding variations that appear amenable to analytical treatment. The first includes plasticity, and the second, viscoelasticity.

Adhesive Debonding of an Elasto-Plastic Plate from a Rigid Substrate.

In another paper, DeVries[25] presents some early results and experimental data, for the debonding of a metal plate strip or beam from a rigid substrate. A bi-material combination is considered, with no interlayer, and deformations of the substrate are neglected. The problem is a direct analog to the first one considered in this paper based upon the classical Obreimoff calculation. Whereas this previous case, and most others encountered in the literature assume elastic deformations and classical beam bending theory - even when the assumptions are patently violated as in a 90 degree bend in a bend! - DeVries has carried through the calculations for a material whose stress-strain curve is assumed to be elastic-purely plastic with the limiting plastic stress being σ_0. While many materials do not

22

completely follow such an ideal non-strainhardening material behavior, the results are important because it exhibits the qualitative effects to be expected due to plasticity, and moreover, has some direct applications to a double pressurized blister test in which, for example, two explosively welded beams or plate strips having an initially small area of central unbonding can be separated. (In principle, if the materials were identical and chemically clean, then the measured adhesive fracture energy between them should approach the cohesive fracture energy in either of the two separately. In some of our tests to date, we have achieved values of γ_a of the order of 90 percent the γ_c values in steel.)

The elasto-plastic analysis proceeds in essentially the same manner as before, with the basic assumption that plane sections remain plane after straining even though the stress distribution changes from linear up to the elastic limit to a truncated triangle as the outer beam fiber, and subsequently the inner fibers, reach the (maximum) yield stress. Figure 8 shows the progressively developing stress distributions across the beam depth. It should be mentioned, incidentally, that it is not necessary for the beam to debond from the substrate, if it is so "soft" that a fully developed plastic hinge develops at the clamped end before the adhesive strength of the bond is reached.

From Figure 8 it is seen that plasticity will develop gradually over the length of the beam beginning at the clamped end, and at any section the central portion near the neutral axis $|y| < \xi$, will be in an elastic state, while near the outer portions $\xi < |y| < h$, will have pure plastic flow. Hence[±] taking the beam thickness as 2b, the moment at a point along the length, x, will be

$$M(x) = 2b \int_{-h}^{h} \sigma_x(x,y) \, y \, dy \qquad (65)$$

$$= 2b \cdot 2 \int_{0}^{\xi} \sigma_x(x,y) \, y \, dy + 2b \cdot 2 \int_{\xi}^{h} \sigma_x(x,y) \, y \, dy$$

$$= 4b \int_{0}^{\xi} E \left[zy \frac{d^2w}{dx^2} \right] y \, dy + 4b \int_{\xi}^{h} \sigma_0 \, y \, dy$$

± To maintain consistency with Reference 25, the notation of 2h and 2b for the thickness and width of the beam is different than in other examples in this paper.

$$= 4b \, E \, \frac{d^2w}{dx^2} \, \frac{\xi^3}{3} + 4b\sigma_0 \, \frac{1}{2} \, (h^2 - \xi^2) \tag{66}$$

where the strain in the elastic portion is $e_x = y \, d^2w/dx^2$, and the stress is constant $\sigma_x = \sigma_0$ for $\xi < |y| \le h$. So assuming that the problem to be solved is an end loaded cantilever beam such that $M(x) = P(\ell - x)$, with the origin of $\underline{x}$ at the bonded end, one has the differential equation for the beam

$$\frac{4Eb}{3} \, \xi^3 \, \frac{d^2w}{dx^2} + 2b\sigma_0 \, (h^2 - \xi^2) = P(\ell - x) \; : \; 0 < x \le x^* \tag{67}$$

which holds in the region $0 \le x \le x^*$, where x^* is the length at which the outer fiber at $y = h$ has just attained the plastic limit, and

$$\frac{Eb(2h)^3}{12} \, \frac{d^2w}{dx^2} = P(\ell - x) \qquad : \qquad x^* \le x \le 1 \tag{68}$$

Continuity of deflection and slope must be maintained at $x = x^*$, and of course a bonded end at $x = 0$ implies that

$$w(o) = dw(o)/dx = o \tag{69}$$

Circumventing the calculation of the deflection and the energies which are given elsewhere, one finds upon deducing the criticality condition in the usual form

$$\frac{\ell I}{\partial \ell} = \frac{\partial U}{\partial \ell} + \frac{\partial}{\partial \ell} \, (\gamma_a \ell) \tag{70}$$

that $\quad \gamma_a = \frac{\partial}{\partial \ell} \, (I - U) = \frac{\sigma_0^2 h}{E} \left[1 - \frac{2}{\sqrt{3}} \sqrt{1 - \frac{P\ell}{2\sigma_0 bh^2}} \right] \tag{71}$

Now if enough load, P_e, is applied to just cause the yield stress, σ_0, to be reached at the outer fiber at the bonded end, i.e., all elastic, then the developed moment at the support can be expressed as

$$\sigma_0 = \frac{P_e \ell h}{\frac{1}{12}(2b)(2h)^3} = \frac{3}{4} \, \frac{P_e \ell}{bh^2} \; ; \; P_e \ell = \frac{4}{3} \, \sigma_0 bh^2 \tag{72}$$

leading to

$$\gamma_a = \frac{\sigma_o^2 h}{3E} \qquad \text{(elastic, compare 8a)} \qquad (73)$$

On the other hand, if a fully developed plastic hinge is developed at the support

$$P_p \ell = 2\sigma_o bh^2 \qquad (74)$$

and in this case (P can never exceed P_p)

$$\gamma_a = \frac{\sigma_o^2 h}{E} \qquad \text{(completely plastic hinge)} \qquad (75)$$

Assuming therefore that debonding does occur prior to exceeding elastic conditions, i.e., $P \le P_e = (4/3)\sigma_o bh^2/\ell$, elastic conditions, (8), will apply; if $P_e \le P \le P_p = 2\sigma_o bh^2/\ell$, then the elasto-plastic formula (71) may be used for an elasto-purely plastic material to measure the adhesive fracture energy.

Our preliminary experiments on bonded bonded aluminum beams have been encouraging, although structural bonding adhesives (3M Co. - 2216B/A) were used rather than explosive welding. Values of $\gamma_a \approx 9 \times 10^5 \text{ergs/cm}^2 = 5 \text{ in-lbs/in}^2$ were obtained in the experiments reported more fully in Reference 25. As emphasized earlier however, the important point to make in this paper is that another engineering material parameter, this time plasticity, can be incorporated quantitatively into a continuum mechanics analysis.

Time Dependent Adhesive Fracture

In none of the examples described to date has it been necessary to introduce explicitly time or temperature dependence of the material properties. In many polymers however, and certain metals at elevated temperatures, these effects can have a profound effect upon cohesive or adhesive fracture. Our present understanding permits some quantitative deductions providing the material behavior is linearly viscoelastic and providing linear viscoelastic material properties are involved. By utilizing a

25

spherical flaw model of a flaw in an incompressible but linearly visco-
elastic medium subjected to uniform external tension, Williams[14] was
able to deduce an exact extension of Griffith brittle fracture theory. It
verified the intuitive feeling that the time dependent critical stress
(σ_{cr}) required to initiate fracture was of the qualitative form

$$\sigma_{cr}(t_f) = k \sqrt{\frac{E^*(t_f) \gamma_c}{a}} \tag{76}$$

where $\underline{a}$ was the flaw size. $E^*(t_f)$ is a time dependent modulus which may be
different for each loading history. However, for qualitative purposes it
may be thought of as a relaxation modulus (Figure 9) which decreases from a
high short time, glassy value (E_g) to a low, long time, rubbery modulus (E_e)
over several decades of time. For a constant value of γ_c, the time to frac-
ture (t_f), would be given implicitly by (76). Since this paper[14], Bennett,
et.al. [26] have shown that γ_c is also time dependent*, which leads one to
suspect that the adhesive fracture energy should also be time dependent.
This latter suspicion has just recently been verified on a polyurethene-
quartz material combination. Hence the expected debonding behavior would be
of the qualitative form

$$\sigma_{cr}(t_f) = k \sqrt{\frac{E^*(t_f) \gamma_a(t_f)}{a}} \tag{77}$$

Theoretical Formulation. In order to describe this time-temperature
dependent fracture within a more formal framework, consider the energy
balance concept within a thermodynamic framework in terms of the power equa-
tion for a continuum[14]. In this form, the meanings of the various con-
tributions are more readily apparent. The conservation of energy requires
that the rate of doing work upon a system, is equal to that absorbed in the
system. Thus one has

$$\dot{I} = \dot{F} + 2\dot{D} + \dot{K} + \dot{\Gamma} \tag{78}$$

---

* Actually reduced time dependent, t/a_T, in which a_T is one WLF time
  temperature shift factor. (See Reference 27)

in which $\dot{I}$ is rate of work input which usually consists of applied forces or displacements at the surface of the body plus any contribution of body forces. Using the notation of Sokolnikoff[17]

$$\dot{I} = \int_S \overset{\nu}{T_i}\dot{u}_i dS + \int_V F_i \dot{u}_i dV \qquad (79)$$

where $\overset{\nu}{T_i}$ are the components of the applied (vector) force $\overset{\nu}{T}$ distributed over the surface (S), F_i the components of any body force over the volume (V), and $\dot{u}_i$ the components of the displacement rate in the ith direction (i = 1, 2, 3).

On the inside of the body, there is the free energy (F), and any dissipation resulting usually from the strain energy of deformation such that

$$\dot{F} + 2D = \frac{d}{dt} \int_V \int_0^t \sigma_{ij}\dot{e}_{ij} dt\, dV \qquad (80)$$

Here σ_{ij} and $\dot{e}_{ij}$ are the components of the stress and strain rate respectively, and it is important to note that at this point no constitutive or stress strain law connecting them has been assumed. If the material is elastic, $\sigma \sim e$; but if for example, it is elastic-plastic or viscoelastic, the appropriate relations can also be inserted into (80). The kinetic energy rate ($\dot{K}$) is expressed as

$$\dot{K} = \frac{d}{dt} \int_V \int_0^t \rho \ddot{u}_i \dot{u}_i\, dt dV = \frac{d}{dt} \int_V \frac{\rho}{2} \dot{u}_i \dot{u}_i\, dV \qquad (81)$$

leaving only the surface energy contribution, Γ, which will be the rate of energy consumed in creating any new fracture surface area

$$\dot{\Gamma} = \frac{d}{dt} \int_S \gamma_{c,a} dS \qquad (82)$$

regardless of its source, where to be specific, the subscript c,a has been added to γ to denote cohesive or adhesive fracture. Thus this term would include not only the energy to break primary bonds, but also secondary chemical bonds as well as any viscous or mechanical work in untangling polymer chains at the fracture surface. The interpretation of either of the

specific fracture energies (γ) is, therefore, the energy required to create new fracture surface area regardless of the source or combination of sources from which it may arise.

Centrally Unbonded Pressurized Viscoelastic Strip. As an example of time dependent adhesive fracture, consider the response of a centrally debonded pressurized strip of linear viscoelastic material[29]. The time dependent deflection (w) of the strip of length 2a(t) can be deduced to be

$$24 \; Iw \; [x,t; \; a(t)] \; = \; L^{-1}[\bar{q}(p)p\bar{D}_{crp}(p)] \; [a^2(t) - x^2]^2 \tag{83}$$

in which L^{-1} indicates an inverse Laplace transform, and $\bar{q}(p)$ and $\bar{D}_{crp}(p)$ indicate Laplace transforms of the time dependent loading per unit width, q(t), and creep compliance, $D_{crp}(t)$ respectively. The center of the strip is at x = 0 and the strip is assumed rigidly clamped at $|x| = a(t)$. The length of the beam, 2a(t) can change with time if debonding occurs at these bonded ends. For this long strip the moment of inertia per unit length, including the plane strain factor of $(1 - \nu^2)$ in the modulus can be expressed as $I = h^3/[12(1 - \nu^2)]$.

From the general theorem (78) as specialized to classical beam theory, one can write the strain energy of deformation (80) as

$$\dot{F} + 2D = 2 \frac{d}{dt} \int_0^{a(t)} \int_0^t M \; [x,\tau; \; a(\tau)] \frac{d}{d\tau} \left[\frac{\partial^2 w \; [x,\tau; \; a(\tau)]}{\partial x^2} \right] d\tau dx \tag{84}$$

in which M is the bending moment in the beam. Hence

$$\dot{F} + 2D = 2 \frac{d}{dt} \int_0^{a(t)} \int_0^t - \frac{q(\tau)}{6} [a^2(\tau) - 3x^2] \frac{\partial}{\partial \tau} \left[- \frac{a^2(\tau) - 3x^2}{6I} \right. $$
$$\left. L^{-1}(\bar{q}p\bar{D}_{crp}) \right] d\tau dx \tag{85}$$

Similarly, the work input to the system is

$$\dot{I} \; = \; 2q(t) \int_0^{a(t)} \frac{\partial}{\partial t} [w(x,t); \; a(t)] \; dx \tag{86}$$

28

assuming the loading is uniformly distributed spacewise. Thereupon neglecting any kinetic energy effects, and writing the change in surface energy rate as

$$\dot{\Gamma} = 2\gamma_a \dot{a} \tag{87}$$

and inserting (85) - (87) into (78), one finds, for $\dot{a} \neq 0$, the integro-differential equation for the determination of the time dependent crack position, $a(t)$.

$$\int_0^t [a^2(\tau) - 3a^2(t)] \, L^{-1} \, \overline{qp}\overline{D}_{crp} \, \frac{\partial}{\partial t} \left\{ q(\tau) \, [a^2(\tau) - 3a^2(t)] \right\} d\tau = 36 I \gamma_a(t) \tag{88}$$

But up to the time of fracture initiation, $t = t_f$, the length of the beam has still not changed from its initial length $a(0) \equiv a_0$, so that one can write

$$\int_0^{t_f} - 2a_0^2 2 \, L^{-1} \, [\overline{qp}\overline{D}_{crp}] \, \frac{\partial}{\partial t} \, [- 2a_0^2 \, q(\tau)] \, d\tau = 36 I \gamma_a(t_f) \tag{89}$$

from which the time to fracture, t_f, is to be deduced. It is apparent that the time to initiation of the unbond will depend upon the history of the pressurization $q(t)$ and the viscoelastic material properties reflected in the creep compliance.

As a simple illustration, assume the pressurization linearly increases with time,

$$q(t) = m t \tag{90}$$

Inserting this loading into (89) and computing the inverse Laplace transform from its convolution integral as

$$L^{-1} \, [\overline{q}(p) \cdot p \cdot \overline{D}_{crp}(p)] = m \, D^{(1)}(t) \tag{91}$$

in which it is convenient to define

29

$$D^{(i+1)}(t) = \int_0^t D^{(i)}(\xi)d\xi \quad ; \quad D^{(o)}(t) \equiv D_{crp}(t) \tag{92}$$

one finds

$$(m \, t_f)^2 = q^2(t)\bigg|_{ramp} = \frac{[18E_g I \gamma_a(t_f)]/a_o^4}{\left[\dfrac{D^{(2)}(t_f)}{D_g t_f/2}\right]} \tag{93}$$

In the case of a very fast rise in pressurization, the debonding
will take place in vanishingly small times for which $D^{(2)}(t_f \to o) \to D_g t_f/2$,
so that

$$q^2 \xrightarrow[\substack{sharp \\ ramp}]{} \frac{18E_g I \gamma_a^g}{a_o^4} = \frac{3}{2(1-\nu^2)}\left(\frac{h}{a_o}\right)^3 \frac{E_g \gamma_a^g}{a_o} \tag{94}$$

which approaches the elastic result, (12). For other, slower loadings, the
character of (93) is as expected from the qualitative considerations because
the creep compliance is approximately the inverse of the relaxation modulus,
and the double integration of the compliance characterization happens to
be that which corresponds to a ramp loading input, i.e., other loading his-
tories give a different number or combinations of integrals of the compli-
ance.

In any event, it has proven possible to include a time dependent
material behavior in the analysis, explicitly, including a time dependent
cohesive fracture energy, t/a_T, as published by Bennett, et.al.[26]; the
authors by an extension of the same technique have also shown a time
dependence in γ_a[28]. It should be noted in passing that the WLF a_T
time-temperature shift factor[27] used in correlating the cohesive fracture
data was the same as that used in correlating the relaxation modulus data.
In the cohesive energy measurements, γ_c was found to vary by a factor of
approximately 50 over six decades of log time[26]. Similar major variations
have been found for the polyurethane-quartz adhesive unbond[28].

It is also possible to deduce a fracture energy from a moving crack,
although to date we have had limited success except on an ad hoc or at
best pseudo-theoretical basis. For monotonic increasing loading in thin
sheets, for example, it appears that plasticity will have to be incorporated
in order to predict finite crack propagation velocities. Further effort
in this area is required because there are certain experimental advantages

30

in deducing the critical fracture energy from photographic measurements of a moving crack as compared to somewhat subjectively deducing the "first" motion of a small pre-cut flaw.

THE PRESSURIZED BLISTER EXPERIMENTAL CONFIGURATION

So far there has been considerable emphasis upon a centrally unbonded infinite plate strip pressurized blister configuration. The reason is mainly because of the relative ease with which the various changes in geometry and materials could be dealt with analytically and thus exhibit the major phenomenological features. From the experimental point of view, however, this configuration is rather poor because of the difficulty in pressure sealing the open ends of the strip. Several other practical matters also impede a simple evaluation of the adhesive fracture energy. First, we have found that it is difficult to construct a specimen for which the adhesive bonding or glue does not accumulate at the crack ends or along the sides of the specimen thus leaving a lump at precisely the point where the debond is to initiate. Also, it is often not easy to control the atmospheric environment surrounding the progressing debond. While these and other practical objections can be overcome, our search for an alternate simple test specimen led to a consideration of the pressurized blister test originally proposed by Dannenburg[30] for the adhesion of paint. A Griffith type energy balance of this geometry, but with a central point loading, was next contributed by Malyshev and Salganik[31]. Our work consisted of combining these two features, i.e., a self centering uniform pressurization specimen and a continuum mechanics energy balance, as into the pressurized blister or circular pancake specimen[32,22].

The Pressurized Blister Test

Paralleling then the development in (9) et.seg., consider therefore a thin elastic disk bonded to a rigid substrate (Figure 10) for which one may write from the principle of energy conservation, that the work done by the applied pressure moving through the virtual displacement must be balanced by the change in internal strain energy plus the change in the energy to create any new surface. Inasmuch as the change in internal energy

31

is one-half the applied work for a linear load-deflection relation by Clapeyron's theorem,[17] one has

$$1/2 \left[2\pi \int_0^a P_0 \; \delta w(r) r dr \right] = \delta(\gamma_a \pi a^2) \qquad (95)$$

From plate theory, one finds that the deflection of a uniformly loaded clamped plate of radius a is given by[16]

$$w(r) = (1/64) \, (p_0/D) \, (a^2 - r^2)^2 \qquad (96)$$

where $D = Eh^3/12(1 - \nu^2)$ is the plate flexural rigidity, so that upon inserting (96) into (95) and calculating the criticality condition, $\partial U/\partial(\pi a^2) = \gamma_a$, one finds

$$\gamma_a = \frac{3(1 - \nu^2)}{32} \; \frac{P_{cr}^2}{E/a} \cdot \left(\frac{a}{h}\right)^3 \qquad (97)$$

It proved experimentally convenient to observe the critical pressure, P_{cr}, at the same instant as the radius increased, thus expressing (97) in the form

$$P_{cr} = \frac{\left\{ 512 Eh^3 \, \gamma_a/[3(1 - \nu^2)] \right\}^{1/2}}{(2a)^2} = \frac{K \gamma_a}{(2a)^2} \qquad (98)$$

which thus leads one to expect a hyperbolic type variation of the experimental data of P_{cr} versus blister diameter squared. Typical results are reproduced in Figure 11; the value of γ_a is deduced from (98) by a best fit of the experimental data.

Actually it may be noted that at the right (lower) end of the curve, there is an apparent departure of the data from the $p \sim (2a)^{-2}$ variation deduced in (98). In point of fact, the data are progressing through a transition toward membrane behavior, as in the strip plate example discussed earlier, (35). Jones[33] has also examined this paint for the circular blisters with which he has experimented, and found a consistent pattern from which a closer agreement with the experimental data can be obtained if warranted.

In addition, we have now had some success with the circular pressurized blister bonded to the substrate through an adhesive interlayer. The plate strip correction factors for interlayers seems to be reproduced, with a bit different numerical values, in the work of Burton, et.al.[22]. Inasmuch as the infinite strip solution emerges in a simple power series in the coordinate with clamped trigonometric functions at worst, i.e., (50) and (52), and the circular plate on an elastic foundation requires at least modified Bessel functions[22], one should verify the necessity for improved correction factors before entering upon the calculations. In any event, the philosophical point is believed established. Should the benefit be sufficient, ever improved continuum mechanics solutions can be developed. For the present purpose, however, the major point to reiterate is the breath of parametric changes with which it is possible to deal, if required.

APPLICATIONS

In the previous discussion, the major emphasis has been upon the analytical and experimental ease with which a technically useful quantity, the potentially time-temperature dependent adhesive fracture energy, $\gamma_a(t/a_T)$, can be measured. It should be recognized however that the end result is not property measurement alone, but to use these data subsequently to analyze other engineering configurations and to be able to predict, a priori, when adhesive debonding will occur. Providing then only that the interface conditions in the new design are identical to the laboratory specimen for which γ_a was measured, e.g., surface roughness, cleanliness, environment, and that numerical complexities of the stress analysis are not insurmountable, which is unlikely in these days of high speed computers, there is no reason why this engineering fracture assessment in Region II can not be made. It should be emphasized that this point is independent of whether or not the physical chemist understands the connection, if any, between the specific fracture energy, γ_a, and the interfacial molecular structure.

33

From an engineering standpoint, this measured γ_a value is more useful than the commonly obtained "peel strength" because as the fracture energy is a fundamental material property, independent of being measured in tension, shear, or torsion, it can be determined once, or as a function of reduced time, t/a_T as required, and then used in the subsequent stress and fracture calculations much like the other material property data, e.g., Youngs' modulus, Poisson's ratio, or tensile strength.

The following examples include some of those with which we have had personal experience and a reasonable amount of quantitative success.

Thermal Debonding of a Rubber Cylinder From its Container

In this case a glass cylinder was filled with a polyurethane rubber having a lower coefficient of thermal expansion than the glass. After curing, the temperature was to be dropped, tending to pull the rubber inward from the container walls and debonding it at the ends. After measuring γ_a for this material combination separately in a pressurized blister test, the predicted design curve showing safe and unsafe operation is shown in Figure 12 and a photograph of the adhesively bonded part is given in Figure 13 where cracks, recorded by X-ray analysis, were observed at the end of the rubber at the glass interface.

Material Shear-out in a Cylinder Under Axial Acceleration

In a somewhat similar geometry except for the tube being steel and the filling being a solid rocket fuel, it was desired to predict the maximum axial acceleration which could be withstood without the fuel debonding from the sides of the cylinder shearing out. Using a separate measurement of γ_a between propellant and steel and the simple analysis given in Reference 34, bounds upon the limiting acceleration could be estimated.

Explosively Bonded Blister Steel Specimens

Through the courtesy of a colleague, Dr. A. A. Ezra, University of Denver, we obtained several explosively welded steel specimens. They were essentially thick cubes approximately one inch on a side to which had been explosively bonded on one side, a thin steel sheet of one-tenth inch in thickness. After carefully tapping through the block perpendicular to the

34

thin plate, pressurized oil was applied through the hole in an attempt
to lift off the sheet in a blister experiment. (Figure 14) After several
tries, a successful technique was developed and an adhesive fracture energy
approaching 90 percent of the cohesive fracture energy ("fracture
toughness") of the steel was attained. A photograph of the sectioned, frac-
tured specimen is shown in Figure 15. In a sense the ratio of γ_a/γ_c could
be viewed as a weld efficiency, although it is too early in our explor-
atory investigations to be definite. A recent report on this subject has
just been presented by DeVries[35].

Evaluation of Dental Adhesives

The analysis of the pressurized blister test was conducted assuming
that plate and/or membrane theory was adequate to handle the stress analysis,
even acknowledging other shortcomings in the analysis. Fortunately, the
block specimen does not contain many of these approximations, and furthermore,
is very appropriate for a series of tests in conjunction with our dental
research. For a very thick (infinite) block of elastic material, an exact
analysis can be made based upon the work of Mossakovskii and Rybka.
(Figure 4b) In this case the adhesive fracture energy between the two
materials can be evaluated as[18]

$$\gamma_a = p_{cr}^2 \ [2(1 - \nu^2)/ \pi] \ (a/E) \qquad\qquad (99)$$

including the effect of the stress singularities. Preliminary work in our
laboratory using the pressurized block, primarily in conjunction with our
dental adhesive evaluation has indicated such an experimental configuration
is feasible. A sketch of the assembly is shown in Figure 16, and the phy-
sical size of the experimental set-up is apparent in Figure 17.

One of the more useful things about this test is its relatively low
cost. Pressure was injected through the small flaw diameter and the γ_a
values for several commercial dental adhesives were measured against teeth,
ivory, and various other synthetic materials of interest in dentistry[36].
It is believed that these data will not only be useful for relative rank-
ings and quality control, much in the same way as "peel strengths" are
used, but that they will have fundamental inherent value when it comes
to evaluate the efficiency of dental adhesion in filling optimized cavity

shapes and assessing the economic advantages of one of the more intangible
variables in the oral cavity. It should not escape the reader that the
pressurizing fluid does not have to be air: environmental effects upon the
bonding efficiency often can be simulated by using oil, inert gasses,
or controlled saline solutions.

By far the most fascinating adhesives project in which we have attempted
to use our pressurized block or blister technique has been in assessing the
relative in vivo efficiency of barnacle cement - attached under water! -
compared to various commercial preparations[37]. With the cooperation of
J. R. Saroyan and E. Lindner at the San Francisco Bay Naval Shipyard we were
able to grow live barnacles over wax filled holes in PMMA sheets. After a
three month submersion in salt water, during which time the barnacles
attached and grew, the recovered specimens and a cross-sectional sketch
are shown in Figure 17. The barnacles were then tested in essentially a
pressurized blister configuration to determine their specific adhesive
fracture energy. In all cases, the adhesive debonding occurred at the PMMA -
barnacle cement interface. Without discussing our detailed results, it may
be noted as a matter of some general interest that the lowly, unsophisticated
barnacle could develop as high an adhesive fracture energy in water as
our best commercial dental cements could obtain under dry conditions!

THE MECHANICS-CHEMICAL INTERFACE

So far this discussion has been entirely upon the continuum mechanics
aspects in order to illustrate the type of analysis which can be conducted,
and provide the chemists with some idea of the parameters with which con-
tinuum mechanics deal. Simultaneously, it is intended to encourage
their interdisciplinary assistance in obtaining, and better understanding,
the appropriate material properties needed by the analyst. Additional
parameters can also be included if the chemist deems them essential in
treating adhesive fracture. It could include for example, anisotropy of
the mechanical properties due to directional properties in rolled metal
or cured polymers. Such factors will oftentimes be mandatory, as for
example in analyzing teeth because of their strongly oriented modular con-
struction. On the other hand, there is no point in becoming too involved
in complexities for their own sake. It is thought more appropriate to

provide physical and polymer chemists with an insight as to what continuum mechanics can offer and await their requests regarding specific missing links they need.

It has been pointed out several times that the mechanics analyst cares little which symbol, γ_c or γ_a, he inserts in his equations, merely noting that the first pertains to fracture in one material, and the second to fracture between two. On the other hand, the engineer faced with the design of an adhesive joint would be aided considerably if someone could furnish him guidelines as to the major interactions or couplings between mechanical properties such as modulus and fracture energy and the molecular composition of the materials involved.

One of the more obvious ones is that known from the theory of rubber elasticity. The long time modulus (E_e) is known to be proportional to the cross-link density of the polymer, (ν_e). Specifically,

$$E_e = 3\nu_e kT \tag{100}$$

in which k is the Boltzmann constant and T the absolute temperature. If similar relations could be developed for more of the material structure parameters, the engineer would have at his disposal direct, albeit sometimes ad hoc, answers which should improve design efficiency.

An Interaction Matrix for Deformation

An attempt has been made in this direction by Kelley and Williams[38-41] in a series of papers dealing with the connection between the chemical structure of polymers and their mechanical properties. The general idea is to introduce an Interaction Matrix shown in tabular form (Table I). It appears that the relaxation modulus and fracture energy, two quantities of major concern to the analyst, can both be approximated by a modified power law representation which is usually applied only to the spectrum of viscoelastic relaxation times $H(\tau)$ controlling the relaxation modulus, i.e.,

$$H(\tau) = \frac{E_g - E_e}{\Gamma(n)} \left(\frac{\tau_0}{\tau}\right)^n \exp\left(-\tau_0/\tau\right) \tag{101}$$

37

which, upon incorporating the time-temperature shift factor, can be converted into the relaxation modulus as

$$E_{rel}(t) = E_e + \frac{E_g - E_e}{[1 + t/(a_T \tau_0)]\, n} \qquad (102)$$

which is shown in a log-log plot in Figure 9. Figure 18 shows data for the relaxation modulus of a typical butadienne rubber, along with the Bennett, et.al.[26] cohesive fracture energy data for the same material.* It is tempting to adopt, at least on an ad hoc basis, a similar representation, for γ_c, namely

$$\gamma_c(t/a_T) = \gamma_e + \frac{\gamma_g - \gamma_e}{[1 + t/a_T \tau_0']^{n'}} \qquad (103)$$

and then inquire as to the sensitivity of the various constants, E_g, E_e, n, τ_0; γ_g, γ_e, n', τ_0'; T_g (glass temperature) to parametric changes in the major chemical parameters such as cross-link density, molecular weight, chain stiffness, etc., and the others enumerated in Table I.

Chain Stiffness and Transition Slope. The success to date has been rather limited, but can be illustrated by at least one example for which an <u>experimental</u> correlation of chemical and mechanical properties has been found - other than the aforementioned <u>theoretical</u> one between cross link density and rubbery modulus, (100). This application, given originally at the Rheology Conference in 1968,[38] proceeded from the Tobolsky[44] observation that the slope of the relaxation modulus through the transition region, n, appeared to be related to the relative stiffness of the polymer chains. In a mechanical sense, "chain stiffness" may be associated with the number of atoms in the chain which would be required to form a circular ring: a few atoms to complete the circle would correspond to a very flexible chain, while a large number of atoms to form a ring would be comparatively rigid.

---

* The similarity between n and n' is rather remarkable and may have more than a coincidental significance. A suitable curve fit to the data of Figure 19 yields, in the form of (103),

$$\gamma_c(t/a_T) = \frac{E_e}{100} + \frac{(E_g/100) - (E_e/100)}{[1 + 10^{3.5}(t/a_T \tau_0')]^n} \qquad (103a)$$

TABLE I

Molecular Characteristics	Symbol	Modified Power Law Parameters				
		E_g	E_e	τ_o	n	T_g
Cross Link Density	ν_e	N	S(1)	N	M	N(2)
Chain Stiffness	N_s	N	N	U	M(3)	S
Monomeric Friction Coefficient	ζ_0	U	N	S(4)	U	S(5)
Solubility Parameter	δ_p	M(6)	N	U	U	S
Molecular Weight	M	N	S(7)	N(8)	N(9)	S(10)
Heterogeneity Index	M_w/M_n	N	N	M	N	M(11)
Molecular Weight between Entanglements	M_e	N	S(12)	N	N	N
Degree of Crystallinity	Λ	N	S	S	S	N(13)
Volume Fraction of Filler	ϕ	N	S	M(14)	S	M
Volume Fraction of Plasticizer	V_p	N	S	S(15)	N	S(16)

U = Unknown, N = Negligible, M = Moderate, S = Strong

Notes for Table I:

(1) Equation (100)
(2) Except at very high values of ν_e
(3) Figure 20
(4) Reference (42)
(5) Reference (43)
(6) References (38), (44)
(7) Effect of entanglements
(8) At high molecular weights
(9) At high molecular weights
(10) At low molecular weights only
(11) Chain end effects from short chain fractions
(12) At high molecular weights producing a plateau or pseudo-equilibrium modulus
(13) Except at very high Λ
(14) Through WLF; Reference (45)
(15) Through ζ_0
(16) Reference (46)

In a quantitative sense, the definition of polymer chain stiffness chosen here is derived from the concept of an "equivalent random link" in the statistical theory of rubberlike elasticity[47,48]. Since actual polymer chains do not have freely orienting backbone bonds, in which each atom-to-atom juncture is completely flexible, an accumulation of the limited flexibility of several bonds may produce a larger chain segment with nearly free orientation of the vector joining the ends of the segment. Those polymers in which the freely orienting segment (equivalent random link) consists of fewer backbone bonds are then considered to be more flexible than those which require a larger number of backbone bonds for free orientation[49]. The number of backbone bonds (atoms) per statistical segment, N_s, is the index of chain stiffness and is determined from

$$N_s = \frac{M_c n_b}{N M_m} \tag{104}$$

where M_c is the average molecular weight of a network chain, n_b is the number of backbone bonds per monomer unit, N is the number of statistical segments per network chain and M_m is the monomer molecular weight. An approximate value for N may be obtained from the maximum extension ratio of the cross-linked polymer, $\lambda_{max} = N^{1/2}$; based on the inverse Langevin function representation of the stress-strain curve by Treloar[47].

In attempting to quantize Tobolsky's observation, a review of the literature revealed that no theoretical relation had been deduced, although the data available from several sources could be combined for such a purpose. Figure 20 contains data on six different unfilled polymers from six sources. One system (polyurethane) contains a variation in basic structure due to systematic changes in catalyst-prepolymer ratio. Accepting for the moment this interaction as being generally valid for all polymers, we can propose an empirical expression for the curve in Figure 20

$$n = 1.5 \left[\ln N_s\right]^{-1} \tag{105}$$

Thus we have the second connection between the chemical and mechanical parameters in Table I; of the 5 x 10 or 50 possible interaction blocks assumed to exist, two have been tentatively filled in!

It is immediately obvious that a significant additional amount of work is yet uncompleted. For the time being however, with the subjective assistance of our colleagues, Table I was filled in with at least qualitative estimates of what are expected to be the more important interactions. Even as it stands, the results have been most useful in guiding the emphasis of our research. It is worth reiterating however, that the main thrust of this philosophical approach does not minimize specific research being presently conducted in either chemistry or mechanics, but represents an attempt to spotlight those areas of interdisciplinary concern where even a small amount of light may improve the engineering result through unexpected synergism.

By way of emphasis, even at the risk of some repetition, a complete idea of the engineering importance of the interaction can be seen by considering the representation of the relaxation modulus in terms of the simple Rouse Theory[42]. As described earlier[38], if the Rouse representation of the relaxation modulus is cast into the form

$$E_{rel}(t/a_T) = E_e \sum_{p=0}^{P} \exp\left(- \frac{\pi^2}{18} \frac{E_e}{n_o} p^2 t\right) \tag{106}$$

which is to be approximated by the modified power law representation (102), then the four parameters in (102) can be approximately associated with the Rouse parameters in the following way

$$E_e = 3\nu_e kT \tag{107}$$

$$E_g = 100 U_o / r_o^3 \tag{108}$$

$$n = \frac{\log E_g/E_e}{\log(\tau_{max}/\tau_{min})} = - \frac{\log[(100 U_o/r_o^3)/3\nu_e kT]}{2 \log P} \tag{109}$$

$$\tau_o = \sqrt{\tau_{max} \tau_{min}} = \frac{6 n_o}{\pi^2 \nu_e kT} \cdot \frac{1}{P} \tag{110}$$

in which U_o is the minimum potential energy at the molecular lattice level at a separation distance r_o between a pair of isolated molecules, n_o is the steady state viscosity at zero rate of shear between the polymer segment and its surrounding medium, and P is the number of equivalent freely orienting

41

segments per molecule. Hence, all the physico-mechanical parameters have been represented in terms of chemical structure ones. It may even be noted that to the extent that the number of backbone bonds (atoms) per statistical segment, i.e., N_s in (104), can be at least qualitatively associated with the Rouse parameter, P, the number of freely orienting segments per molecule, the empirical introduction of our inverse logarithmic dependence in (105) is appropriate.[*]

An Interaction Matrix for Fracture

In the foregoing illustration of the Interaction Matrix, the primary emphasis was placed upon the influence of the time-dependent relaxation modulus upon the deformation mechanisms in a polymer. If for illustrative purposes we suppress for the moment the apparently similar time dependence of the cohesive[(26)] and adhesive[(28)], the fracture energy found by Bennett, et.al., we would expect from (76) that the critical stress to induce Region II cohesive fracture, would be

$$\sigma_{cr}(t_f) = k \sqrt{\frac{E^*(t_f)\gamma_c}{a}} \tag{76}$$

where it is to be recalled that $E^*(t_f)$ has the character of a relaxation modulus. The introduction of (107) - (110), or more precise relations from the Interaction Matrix, would then permit a calculation of the direct dependence of the critical fracture stress (σ_{cr}) upon the chemical structure, viz.,

$$\sigma_{cr}(t_f) = k \left[\frac{E_{rel}(E_g, E_e, n, \tau_0; T_g) \gamma_c}{a}\right]^{1/2} \tag{111a}$$

---

[*] It should be clearly understood at this point that N, the number of equivalent random links per chain in the theory of rubberlike elasticity is not the same as P, the number of Gaussian sub-molecules per chain in the Rouse theory. If, however, we assume that P is proportional to the molecular weight M[50], i.e., $P_i = K_0 M_i$ for a molecule containing i monomer units, we must conclude that P is proportional to N, since $N_i = K_1 M_i$. Now K_0 is usually taken at the limit $K_0 \to \infty$, meaning the molecules are infinitely flexible even at a very small molecular weight. According to Peticolas[(50)], a finite value of K_0 would lead to stiffer chains. This would indicate from Equation (109) that at decreasing values of P, i.e. stiffer chains, n should be increased. This is in contradiction to the observed data as seen in Figure 20. This contradiction probably arises from the inadequacy of the sub-molecule model when the Rouse theory is applied to times shorter than those associated with τ_{max}. Recent unpublished refinements of the theory should provide a more reasonable description of bulk polymer behavior over a wider range of conditions.

42

$$= k \left[\frac{E_{rel}[U_0,\ r_0,\ \nu_e,\ P(\text{or } N_s),\ \eta_0 : T_g]\ \gamma_c}{a} \right]^{1/2} \qquad (111b)$$

$$= F\ [U_0,\ r_0,\ \nu_e,\ P(\text{or } N_s),\ \eta_0;\ T_g,\ \gamma_c] \qquad (111c)$$

and thus in principle, would permit the mechanics analyst and the chemist to jointly appreciate the quantitative interaction between their fields.

Before concluding the discussion of this point, however, it is obvious that the previous philosophical objective can be extended - to include the dependence of the specific fracture energy, be it γ_c or γ_a, upon the properties of the material. One could therefore assume the validity of the semi-empirical relation (103) and seek theoretical or empirical relations between the modified fracture power law parameters γ_g, γ_e, n', and τ_0' and the chemical structure. The analog to (76) would be (77) which when expressed in terms of (103) would lead to the analog of (111a),

$$\sigma_{cr}(t_f) = k \left\{ \frac{E_{rel}[E_g,\ E_e,\ n,\ \tau_0;\ \gamma_g,\ \gamma_e,\ n',\ \tau_0' : T_g,\ t_f]}{a} \right\}^{1/2} \qquad (112a)$$

and a "Rouse Theory" or Interaction Matrix for fracture would be required to deduce a generalized fracture expression, say (112b), analogous to (111b).

As reported at this meeting last year[41], a start has been made. From the phenomenological standpoint it seems appropriate to inquire first if the fracture energy would be expected to depend upon the same or different molecular properties as the relaxation modulus. Because it has not been commonly appreciated that both the modulus and fracture energy may independently be time dependent, experiments which have measured, for example, time dependent fracture stress have attributed the time dependence to the "tear energy" with a constant modulus[51]. On the other hand, Williams' analysis[14] assumed the entire dependence lay in the modulus, with a constant fracture energy. Thus one must beware of previous intuition which has perhaps been conditioned by a knowledge of only the time-dependent product, i.e., $\sigma_{cr}(t)$, when in fact it can arise from either or both the modulus and fracture energy. This line of reasoning suggests that from the energetic approach the deformation sensitive quantities are reflected in

43

the modulus while the rupture or bond breakage is reflected in the fracture energy, with the overall breaking stress characteristics being proportional to the product of their respective square roots. From the basic molecular structure viewpoint, however, in the quantum mechanics sense, such a complete partitioning of the individual effects seems unlikely. Hence an Interaction Matrix construction as shown in Table II is probably more appropriate.

Interactions occupying only the U, V, and W blocks along the main diagonal represent mutually independent behavior such that there would be no connection between deformation, cohesion, or adhesion as far as molecular parameters were concerned. As this behavior seems unlikely, provision for off-diagonal interaction is provided, although zeroes can always be entered where appropriate. The additional molecular descriptors V_m and W_n are those needed to account specifically for quantities entering only fracture and not deformation. At the present time the only characteristics we choose to place in this category are the chemical bond energies themselves. On the other hand, several sources suggest, for example, that the molecular weight and cross link density have a direct bearing on cohesive fracture energy,* γ_c.

<u>Molecular Considerations</u>. Benbow[52] reports that there is a hundred-fold increase in energy in polystyrene as the molecular weight, $\bar{M}_w$, is raised from 60,000 to 260,000. These conclusions have been substantiated by Broutman and Kobayashi[53] who report the following values deduced from splitting a tapered cantilever beam

$\bar{M}_w$	γ_c (ergs/cm^2)
53,211	3.5×10^3
231,000	4.3×10^5
246,148	4.0×10^5

---

* Note, however, that according to our previous remarks, it may be important to reassess the basic experimental data to ascertain that the $\bar{M}_w$ and ν_e influence attributed by the referenced authors to γ_c, could not equally as well have been attributed to the modulus.

44

TABLE II

Mechanical Molecular Parameters	Deformation Parameters E_e E_g n τ_o T_g	Fracture Parameters	
		γ_c	γ_a
U_1 U_2 . . . . U_s	U		
V_1 V_2 . . . V_m		V	
W_1 W_2 . . . W_n			W

Berry[54] has suggested that the increase in fracture energy is due to the greater degree of involvement of the longer chains (higher molecular weight) in the plastically deformed area surrounding the crack tip. The least amount of energy is dissipated if the chain is short enough to be completely enclosed by the plastic enclave. Intermediate energy is absorbed if the chain is partly inside and partly outside the region, while maximum energy results if the chain passes through the plastically deformed enclave and both chain ends terminate in the elastic region.

Broutman and Kobayashi[53] also examined the effect of cross-linking in polystyrene, accomplished by gamma radiation using a Cobalt 60 source in order not in introduce a second, and possibly complicating, cross-linking chemical species. At molecular weights of approximately 250,000, the fracture energy was reduced by one-half after a dosage of 50 megarads.

The above typical results suggest a S (strong) interaction for molecular weight and cross linking[±] with weaker and indeterminate effects attributed to the remainder of the molecular parameters in the extended Interaction Matrix, except for the inclusion of chemical bond energies as the V_m and W_n.

If the most gross correlation of the relaxation and fracture data were to apply, i.e., constant proportionality*, then

$$\gamma_c(t) = \mu E_{rel}(t) \tag{113}$$

and simultaneous measurement of E and γ_c would only be required at one time. For example, in the rubbery or elastic long time region,

---

[±] In a private communication, J. R. Kinloch has obtained indications that there would be no effect of molecular weight on γ_c if, for molecular weights between cross links in the range 4000-14,000, the data were reduced to the same glass transition temperature.

* Such a hypothesis would lead to the not unreasonable conclusion that the critical fracture stress $\sigma_{cr}(t_f)$ would be essentially proportional to the first power of the modulus, i.e., $\sigma_{cr} \approx \sqrt{E_{rel}} \cdot \mu E_{rel}/a \approx E_{rel}$, or equivalently, a strain criterion for fracture, $\epsilon_{cr} \approx \sigma_{cr}/E_{rel} \approx \mu'$, which expression has certain similarities to failure in metals.

46

$$\gamma_c(\infty) \equiv \gamma_{ce} = \mu E_e = 3\mu\nu_e kT \text{ or } \mu = \gamma_{ce}/3\nu_e kT \qquad (114)$$

which might be further related to molecular weight or cross-link density through the relationships proposed by Benbow[52] or Brontman and Kobayashi[53], thus eliminating any further need for V_m or W_n quantities in the Inter-action Matrix, or our proposed additional dependence of γ upon chemical bond energy. These matters have proven quite interesting and intriguing to us on strictly an ad hoc basis - sufficiently so to encourage further study upon a more fundamental basis.

Accepting for the moment the analogy suggested in Figure 19 and the above discussion relating the relaxation and fracture energy spectra, we may construct an Interaction Matrix for fracture similar to that described for the modified power law representation of the relaxation modulus. The purpose of such an exercise, to reiterate our earlier remarks, is to gain perspective on known relationships and to point out possible significant interactions for further study.

Time dependent fracture has been observed for both unfilled and filled polymers[55,56,57]. The remarkable feature of this time dependence has been the good agreement between the temperature dependence of the shifting factor a_T, for both small deformation response and large deformation fracture[26]. Since the molecular interpretation of a_T is based on small-scale motion of molecular segments, which is dominated by the temperature difference above the glass temperature $(T-Tg)$[58], these same local segmental motions apparently govern the time dependence of fracture. Most current molecular theories presume an ordering of the polymer chains in front of the advancing crack in which several chain segments are oriented perpendicular to the direction of propagation. This process dissipates considerable energy since it is opposed by the ordinary viscous forces which restrict chain motion, i.e., segmental friction - including chain entanglement. Of course, cross-linking would be expected to increase the difficulty of orientation and contributes additional relaxation mechanisms in the long time portion of the spectra.

This view would support the connection between the relaxation and frac-ture curves at longer times or higher temperatures. Since the maximum

dissipation observed in cyclic (small strain) tests corresponds with the transition region of the relaxation curve, one would expect increasing fracture energy when moving to this experimental time scale from the longer times[63]. At very short times the dissipation is greatly reduced since the material exhibits glassy behavior, but the critical stress is so high that the onset of crack growth would be governed by other factors such as Van der Waal's bonding forces[64], or more likely, the greater number of primary chain backbone bonds holding the load in a given cross-section[62 p.263].

A limiting critical fracture stress or fracture energy in the glassy region of the fracture spectrum seems quite likely, although the data are far too limited for generalization at present. It does appear, however, that the long time, rubbery region has been given sufficient attention for early speculation on the nature of chemical interactions. Lake and Thomas[58] have advanced certain molecular explanations for a limiting tearing energy, T_o, which is largely independent of viscoelastic processes and varies slightly with chemical structure. In this case T_o might be considered roughly equivalent to γ_e, and the reported values for the two quantities for similar polymers agree rather well (Lake and Thomas 10^5 ergs/cm^2 for butadiene-acrylonitrile copolymer and Bennett, et.al.[26], 1.3×10^5 ergs/cm^2 for butadiene-acrylonitrile-acrylic acid terpolymer.) Lake and Thomas derive the following relationship for T_o:

$$T_o = (3/8)^{1/2} g \ell U N \bar{n}^{3/2} \tag{115}$$

where g is the stiffness factor related to our notation N_s by $N_s = g^2 n_b$, ℓ is the length of a monomer unit and is proportional to n_b, U is the energy required to rupture a backbone bond, N is the number of network chains per unit volume, and $\bar{n}$ is the average number of monomer units per chain. Although Lake and Thomas indicate that there is experimental evidence that the type of cross-link has some effect on the variation of T_o with cross-linking, Equation (115) may provide an initial basis for some important interactions between molecular structure and γ_e in Table III.

One of the most interesting features of Figure 19 is the displacement of the fracture transition region along the time scale by three and one-half decades as compared to the relaxation curve. It leaves open the question of a possible generality of shifts to longer times for fracture

TABLE III

Molecular/Microstructural Characteristics	Symbol	Modified Power Law Parameters				
		γ_g	γ_e	τ_o	n	T_g
Cross Link Density	ν_e	M(1)	S(2)	N	M	M(3)
Chain Stiffness	N_s	N	M(4)	U	M(5)	S
Monomeric Friction Coefficient	ζ_o	U	U	S(6)	U	S
Solubility Parameter	δ_p	S	M	U	U	S
Molecular Weight	M	N	S(8)	N(9)	N(10)	S(11)
Heterogeneity Index	M_w/M_n	N	N	M	N	M(12)
Molecular Weight between Entanglements	M_e	N	S(13)	N	N	N
Degree of Crystallinity	Λ	U	S	S	S	N
Volume Fraction of Filler	ϕ	S	S	M(14)	S	M
Volume Fraction of Plasticizer	V_p	S	S	S(15)	N	S(16)

U = Unknown, N = Negligible, M = Moderate, S = Strong

Notes for Table III:

(1) Reference (53)
(2) Reference (58)
(3) References (59), (60)
(4) Reference (58)
(5) Figure 20
(6) Reference (42)
(7) Reference (43)
(8) Effect of entanglements
(9) At high molecular weights
(10) At high molecular weights
(11) Reference (61)
(12) Low M fractions may plasticize (62)
(13) Plateau effect similar to cross-linking
(14) Reference (25) related to T_g
(15) Plasticizer effect on T_g and ζ_0
(16) Reference (46)

of various polymers. The position of τ_0 should be determined to a large degree by the glass transition temperature, T_g. Since the fracture process implies very large strains at the tip of the crack at τ_c, therein could be the principal reason for differing time scales between the fracture energy transition and the small strain relaxation transition. Some evidence is available on the effect of strain induced anisotropy on T_g[65,66] as well as the basic nonlinearity of the response due to finite strains[67]. However, any further examination of this behavior must await the accumulation of experimental fracture data on other polymers. (Smith and Dickie[68] have recently examined a_T-strain effects.)

Table III has therefore been filled in by assuming a correspondence between the relaxation and fracture behavior of polymers. The inter-actions with various molecular and microstructural features were assumed to be similar with respect to the highly time-dependent phenomena, parti-cularly those associated with the transition regions. Some information on the fracture of glassy polymers clearly indicates a dependence of γ_g on cross-linking[53] and molecular weight[52]. Certainly, many of the interactions assumed by analogy in Table III must be checked out experimentally, and quantitative associations should be developed. In any case, the arrange-ment of parameters in an array such as that provided by the Interaction Matrix leads to a more direct assessment of the significance of molecular variations with respect to the deformation and fracture requirements of a polymeric material in its ultimate engineering application.

50

CONCLUSION

Because of the growing technological need for a more cooperative effort between continuum mechanics and physical chemistry in order to improve the quality and understanding of adhesive bonds, this paper has attempted to describe how adhesive failure would be treated from the standpoint of a stress analyst. Two complimentary fracture criteria are involved depending upon the size and distribution of inherent flaws in the vicinity of the interface. In the more probable case of Region II or flaw controlled failure, there are essentially two deformational mechanical property descriptors required, e.g., shear modulus and bulk modulus, which for rubbery (incompressible) polymers can be reduced to a relaxation modulus. In addition, there are the specific fracture energies of cohesion of the individual component materials and of the adhesive interfaces.

With some minor reservations regarding the geometry of the assembly because it affects the accuracy of predicting the stress and strain fields in a practical computational sense, there are only two major impediments to a technologically satisfactory solution to adhesive bonding problems. First, it is necessary to know the size and location of any above average size initial or inherent flaws in the part in order that an appropriate mechanics analysis can be made. Massive, opaque, or inert parts give problems because present non-destructive testing (NDT) techniques are not wholly satisfactory. Second, in the absence of further help from the chemist, a mechanics analyst presently relies upon the similarity of conditions in his test specimen and engineering prototype as far as surface preparation and bonding conditions are concerned. Then the fracture energies measured in the laboratory can be used to predict fracture in other configurations of the same material combinations - without any knowledge of the chemistry involved!

Hence, the second part of this review has been directed toward encouraging a better fundamental understanding of those chemical structure parameters which control or influence the deformation and fracture energy descriptors. In this way it is hoped that a technical knowledge of one interface situation can be extrapolated to a somewhat different one without the

necessity for extensive additional testing. It is believed that here, cooperation between mechanics and chemistry is essential, and for discussion purposes, the idea of an Interaction Matrix has been reiterated as a possible approach.

There is one additional complexity that requires comment, and its brevity should not detract from its importance. Somewhere between the levels of continuum mechanics and quantum mechanics, it seems reasonable to anticipate a working hypothesis associating the cohesive fracture energies $\gamma_c^{(1)}$ and $\gamma_c^{(2)}$ of two solid materials and their combined adhesive fracture energy $\gamma_a^{(1,2)}$, e.g., $\gamma_a^{(1,2)} = (\gamma_c^{(1)} \cdot \gamma_c^{(2)})^{1/2}$ for certain cases of dispersion controlled interactions. Indeed Good, Fowkes and others[73,74] are intimately involved in this subject, and the latter author has published a fairly recent paper whose title "Calculation of the Work of Adhesion by Pair Potential Summation" neatly emphasizes the missing link as far as the continuum mechanics interest is concerned.

Thus while temporarily the mechanics analyst can circumvent a physics-chemical understanding of adhesion by similarity testing, such as using the pressurized blister or block specimen, additional contributions from the chemists on even an ad hoc basis showing reasonably quantitative associations between cohesive and adhesive fracture energy, albeit with "interfacial environmental" qualifications, would be most welcome.

ACKNOWLEDGEMENT

REFERENCES

1. DeBruyne, N. A., Adhesion and Adhesives, Elsevier, Amsterdam, 196 (1951).

2. Goland, M. and Reissner, J. Appl. Phys., 11, 417 (1944).

3. Patrick, R. L. (ed.), Treatise on Adhesion and Adhesives, Marcel Dekker, Ind., New York (1967).

4. Ripling, E. J., Mostovoy, S., and Patrick, R. J., Recent Developments in Adhesive Science, ASTM STP 360, 5 (1964).

5. Griffith, A. A., Proceedings 1st International Congress Applied Mechanics, Delft, 55 (1924).

6. Williams, M. L., J. Appl. Mech., 24, 1, 109 (1957).

7. Williams, M. L., Proceedings 5th U. S. Congress Applied Mechanics, Minneapolis, 451 (1966).

8. Williams, M. L., Proceedings 1st U. S. Congress Applied Mechanics (1951).

9. Williams, M. L., J. Appl. Mech., 19, 526 (1952).

10. Williams, M. L., and Owens, R. H., 2nd U. S. Nat. Congr. Appl. Mech., 407 (1954).

11. Williams, M. L., and Chapkis, R. L., 3rd U. S. Nat. Congr. Appl. Mech., 281 (1958).

12. Williams, M. L., Bull. Seismol. Soc. Amer., 49, 199 (1959).

13. Williams, M. L., and Schapery, R. A., Int. J. Fract. Mech., 1, 64 (1965).

14. Williams, M. L., Int. J. Fract. Mech., 1, 292 (1965).

15. Obreimoff, J. W., Proceedings Royal Society, (London) A 127, 290 (1930).

16. Timoshenko, S. P., and Woinowsky-Krieger, S., Theory of Plates and Shells, McGraw-Hill, New York (1959).

17. Sokolnikoff, I. S., Mathematical Theory of Elasticity, McGraw-Hill, New York (1956).

18. Mossakovskii, W. I., and Rybka, M. T., PMM 28, 1061 (1964).

19. Williams, M. L., J. Appl. Mech., 458-464, Dec. (1955).

20. Williams, M. L., J. Appl. Mech., 251-258, June (1958).

21. Williams, M. L., J. Appl. Polym. Sci., 14, 1121 (1970).

22. Burton, J. D., Jones, W. B., and Williams, M. L., Trans. Amer. Soc. Rheology, Feb. 2-4, 1970, Pasadena, Calif. (to be published).

23. Williams, M. L., UTEC DO 71-037, University of Utah, February 1971.

24. Paris, P. C., and Sih, G. C., ASTM STP 381 (1965).

25. Chang, M. D., DeVries, K. L., and Williams, M. L., The Elasto-Plastic Debonding of a Metal Strip from a Rigid Substrate, University of Utah, DO 71-078, April (1971).

26. Bennett, S. J., Anderson, G. P., and Williams, M. L., J. Appl. Poly. Sci., 14, 735 (1970).

27. Williams, M. L., AIAA Journal, 2, 785 (1964).

28. Bennett, S. J., Anderson, G. P., and DeVries, K. L, unpublished (1971).

29. Williams, M. L., UTEC DO 71-044, University of Utah, January (1971).

30. Dannenberg, H., J. Appl. Polym. Sci., 5, 125 (1961).

31. Malyshev, B. M., and Salganik, R. L., Int. J. Fract. Mech., 1, 114 (1965).

32. Williams, M. L., J. Appl. Polym. Sci., 13, 29 (1969).

33. Jones, W. B., Dissertation, University of Utah (1970).

34. Kunio, T., and Williams, M. L., Proceedings of the 8th Int. Sym. on Space Tech. and Sci., Tokyo (1969).

35. DeVries, K. L., Luntz, R. D., and Williams, M. L., 3rd Int. Conf. on High Energy Forming, Vail Colorado, June (1971)

36. Williams, M. L., Luntz, R. D., DeVries, K. L., and Despain, R. R., UTEC DO 70-196, University of Utah, Dec. (1970) (Int. Assn. Dental. Res., 49th General Meeting, Chicago)

37. Despain, R. R., DeVries, K. L., Luntz, R. D., and Williams, M. L., UTEC DO 70-195, University of Utah, Dec. (1970) (Int. Assn. Dental Res., 49th General Meeting, Chicago)

38. Williams, M. L., and Kelley, F. M., Proc. 5th Int. Cong. Soc. Rheol., 185-202, Oct. (1968) (University of Tokyo Press, 1970).

39. Kelley, F. M., and Williams, M. L., Rubber Chem. Tech., 42, 3 (1969).

40. Williams, M. L., and Kelley, F. M., CPIA Pub. 193, 1, Johns Hopkins University, (APL), 89-105, March (1970).

41. Kelley, F. N., and Williams, M. L., American Chem. Soc., Chicago, Sept. (1970). (UTEC TH 70-148, University of Utah, Aug. 1970).

42. Rouse, P. E., J. Chem. Phys., 21, 1272 (1953).

43. Bueche, F., J. Chem. Phys., 20, 1959 (1952); 25, 599 (1956).

44. Tobolsky, A. V., Properties and Structure of Polymers, John Wiley & Sons, Inc., New York (1960).

45. Landel, R. F., Trans. Soc. Rheol., 2, 53 (1958).

46. Kelley, F. N., and Bueche, F., J. Poly. Sci., 50, 549 (1961).

47. Treloar, L. R. G., The Physics of Rubber Elasticity, 2nd ed., Clarendon, Oxford, (1958).

48. Kuhn, W., Kolloid Z., 76, 258 (1936); 87, 3 (1939).

49. Kelley, F. M., Dissertation, University of Akron (1961).

50. Peticolas, W. L., Rubber Chem. Tech., 36, 1422 (1963).

51. Greensmith, H. W., and Thomas, A. G., J. Poly. Sci., 18, 189 (1955).

52. Benbow, J. J., Proc. Phys. Soc. (London), 78, 970 (1961).

53. Broutman, L. J., and Kobayashi, T., ACS Polymer Preprints 10, Sept. (1969).

54. Berry, J. P., J. Poly. Sci., 2, 4069 (1964).

55. For review of the subject, see B. Rosen, ed., Fracture Processes in Polymeric Solids, John Wiley & Sons, Inc. (1964).

56. Bueche, F., and Halpin, J. C., J. Appl. Phys., 35, 36 (1964).

57. Andrews, E. H., Fracture in Polymers, American Elsevier, New York (1968).

58. Lake, G. J., and Thomas, A. G., Proc. Roy. Soc. A, 300, 1460 (1967).

59. DiMarzio, E. A., J. Res. NBS, 68A, 611 (1964).

60. Nielsen, L. A., Cross-Linking Effect on Physical Properties of Polymers, Washington University/ONR/ARPA Report HPC 68-57 (1968).

61. Fox, T. G., and Flory, P. J., J. Appl. Phys., 21, 581 (1950).

62. Bueche, F., Physical Properties of Polymers, John Wiley & Sons, Inc., New York (1962).

63. Mullins, L., Trans. Inst. Rubber Ind., 35, 213 (1959).

64. Berry, J. P., J. Poly. Sci., 50, 107 (1961).

65. Polmanteer, K. E., Thorne, J. A., and Helmer, J. D., Rubber Chem. Tech., 39, 1403 (1966).

66. Gee, G., Hartley, P. N., Herbert, J. B. M., and Lanceley, H. A., Polymer 1, 365 (1960).

67. Warnaka, G. E., and Miller, H. T., Rubber Chem. Tech. 37, 1421 (1966).

68. Smith, T. L., and Dickie, R. A., J. Poly. Sci., A2 7, 635 (1969).

69. Tobolsky, A. V., and Catsiff, E., J. Poly. Sci., 19, 111 (1956).

70. Landel, R. F., and Fedors, R. F., JPL Space Programs Summary 37-36, IV, Jet Propulsion Laboratory, 137 (1965).

71. Landel, R. F., California Institute of Technology Report, CHECIT PL 68-1, June (1968).

72. Ninomiya, K., and Fujita, H., J. Coll. Sci., 12, 204 (1957); J. Poly. Sci., 24, 233 (1957); J. Phys. Chem., 61, 814 (1957).

73. Girifalco, L. A., and Good, R. J., J. Phys. Chem., 61, 904 (1957).

74. Fowkes, F. M., J. Coll. Interface Sci., 28, 493 (1968).

75. Williams, M. L., Proc. 9th Conf. Adhesion and Adhesives, City Univ. London, April (1971) (UTEC DO 71-068, University of Utah, April 1971).
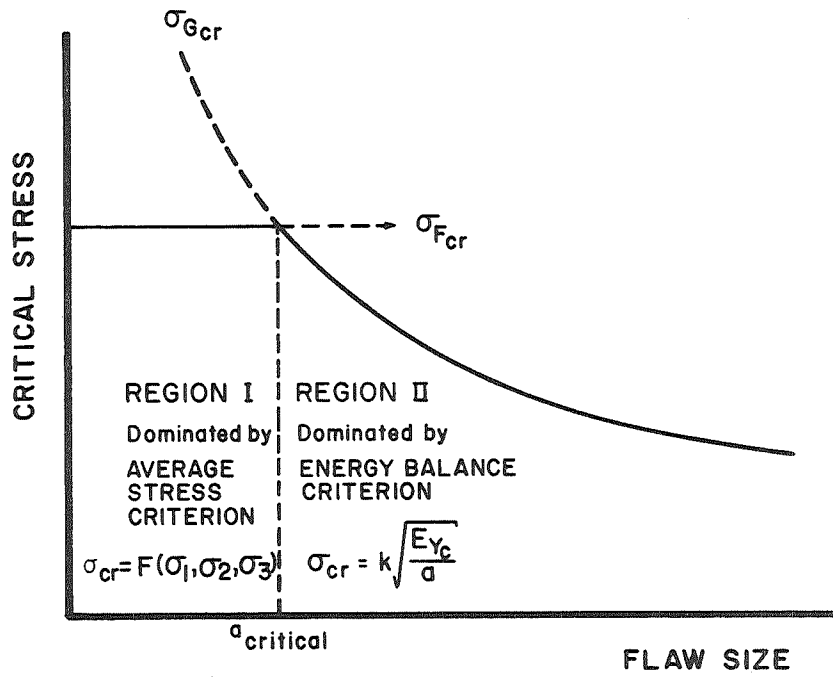
Figure 1. Dominant fracture regions depending upon inherent
flaw size.

Boundary Conditions: $|x| > a$

(1) $v(x,o) = o$

(2) $\tau(x,o) = G[\partial u(x,o)/\partial y + \partial v(x,o)/\partial x] = o$
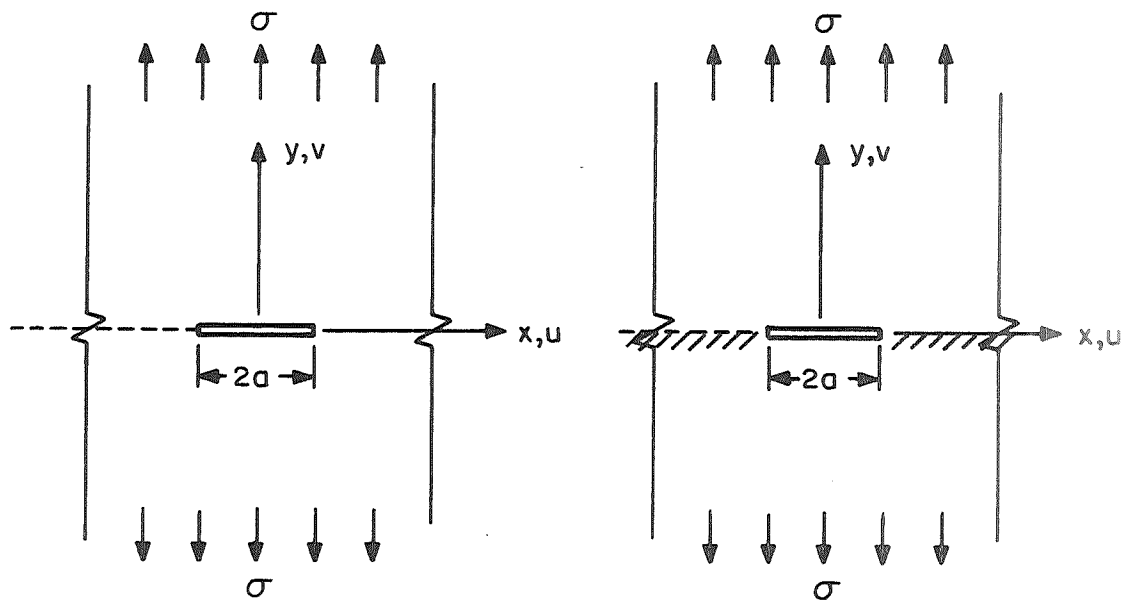
    or because of (1), equivalently,

(2a) $\dfrac{\partial u(x,o)}{\partial y} = o$

Figure 2a. Cohesive fracture

$$\sigma_{cr} = \sqrt{\frac{2}{\pi} \frac{E\gamma_c}{a}} \qquad (5)$$

Boundary Conditions: $|x| > a$

(1) $v(x,o) = o$

(2) $u(x,o) = o$

Figure 2b. Adhesive Fracture

$$\sigma_{cr} = \sqrt{\frac{2}{\pi} \frac{E\gamma_a}{a}} \qquad (6)$$

Figure 2. Comparison of essential boundary conditions for cohesive and
adhesive fracture. The difference is slight and concerns only
whether the lateral displacement, $u(x,o)$, or its normal
derivative, $\partial u(x,o)/\partial y$, is prescribed. Both sets of boundary
conditions lead to singular stresses (References 9, 12)
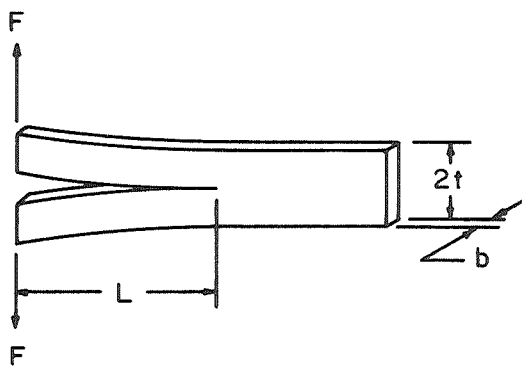
Figure 3. Double cantilever cleavage specimen.
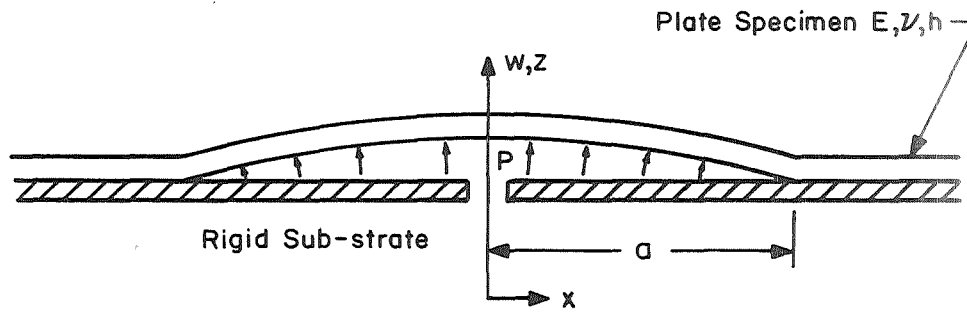
Figure 4a. Pressurized blister specimen.
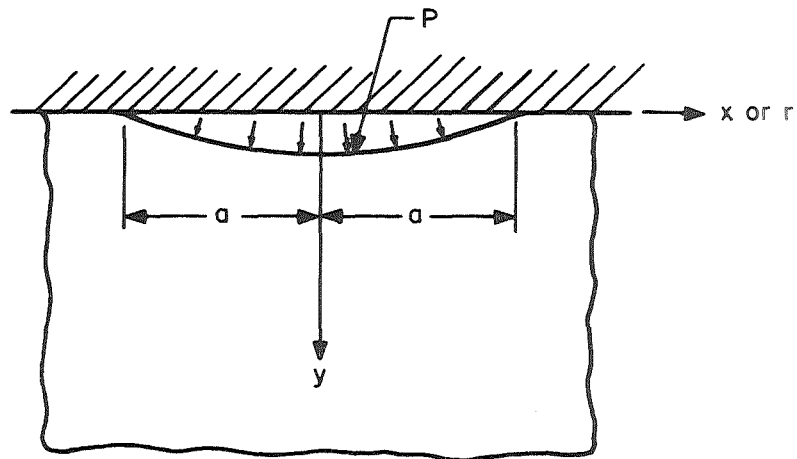
Figure 4b. Pressurized block specimen with penny-
shaped circular flaw or infinite strip
central unbond.

61
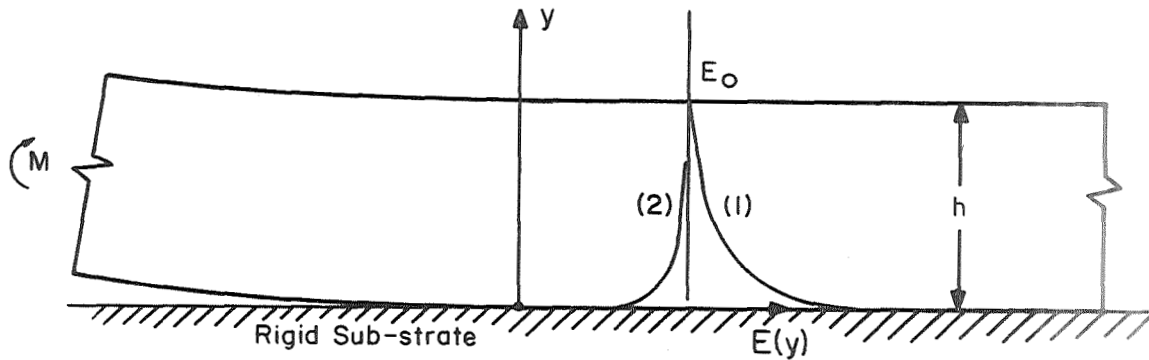
Figure 5a. Skin effect modulus variation $E(y) = E_0 + E_1 \exp(-\lambda y/h)$
Curve (1) shows $E_1 > 0$, curve (2) shows $E_1 < 0$.

$$\left[\frac{g(\lambda, E_1/E_0)}{1 + (E_1/E_0)} \right]^{\frac{1}{2}} = S$$

$\lambda = 10$

$\lambda \Rightarrow \infty$

E_1 / E_0
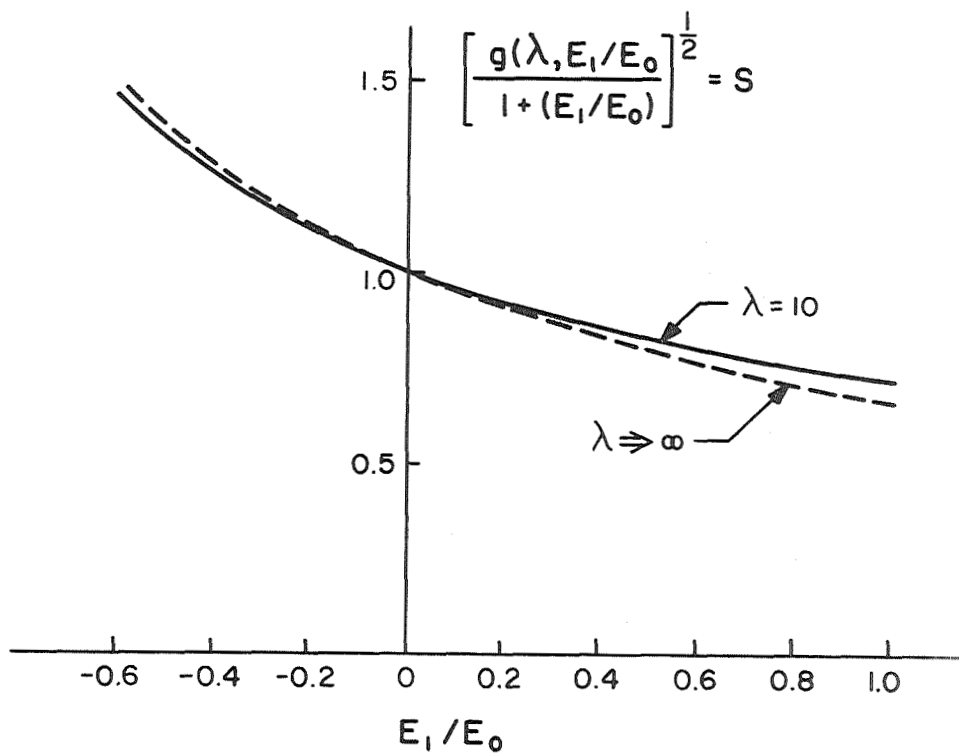
Figure 5b. Effect on increasing critical stress S times due to skin effect modulus.
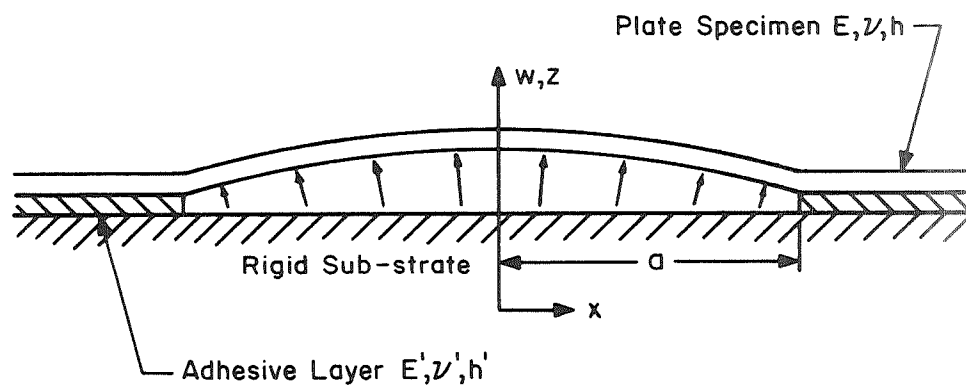
Figure 6.   Blister specimen with finite thickness adhesive interlayer (Reference 21).
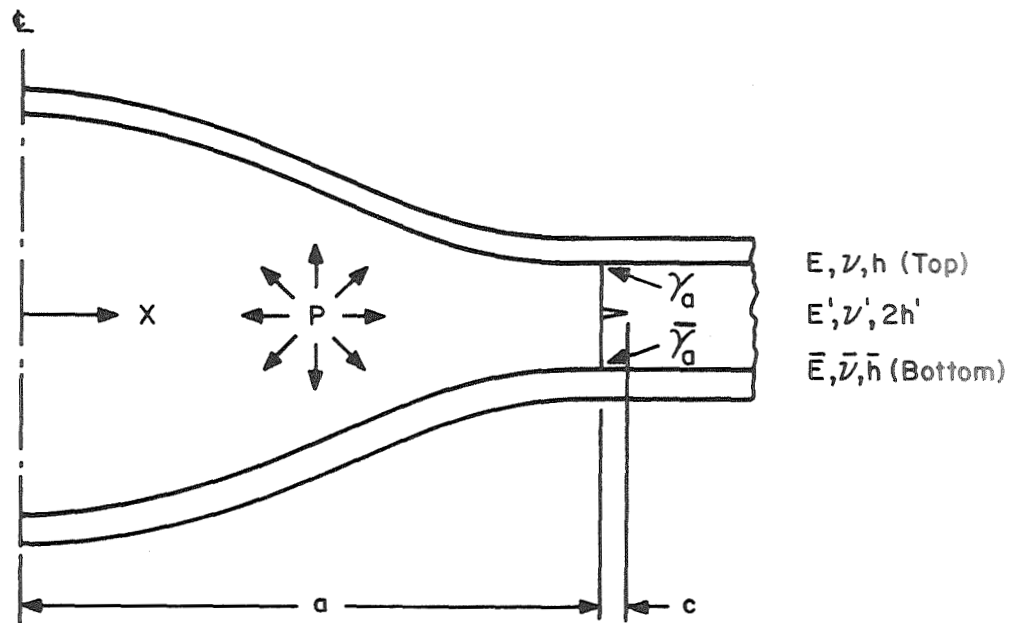
Figure 7. Geometry of the three layer pressurized infinite strip
(Reference 23)
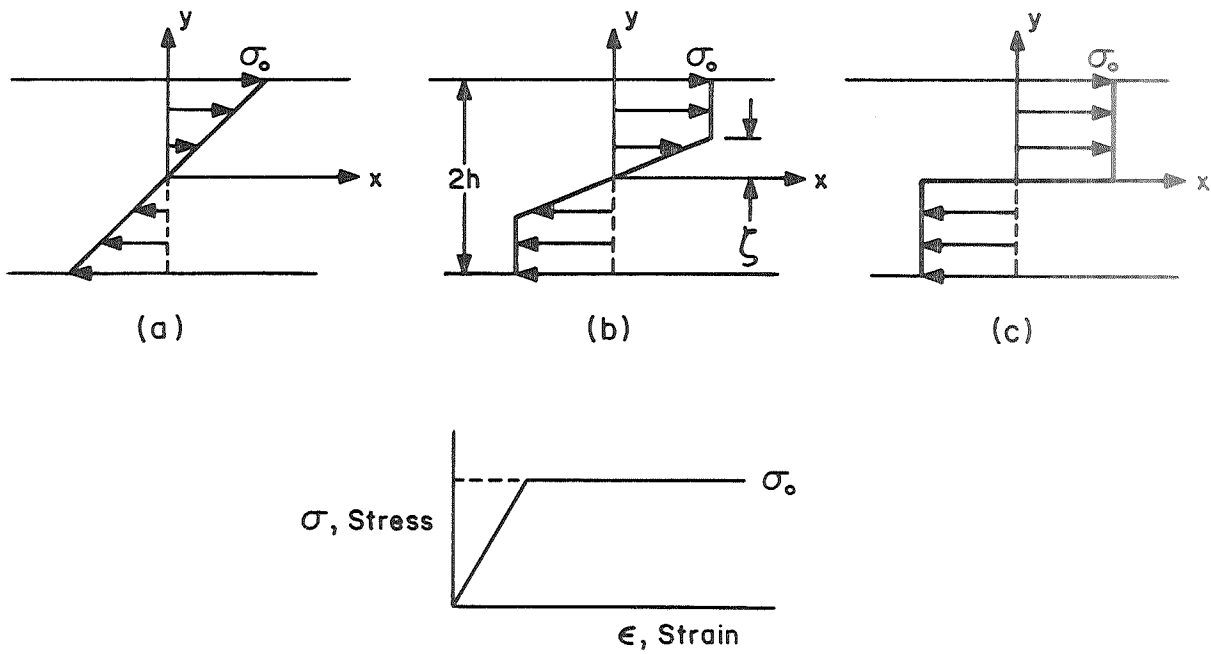
Figure 8. Development of elasto-plasticity through the depth of a beam:
(a) elastic, (b) elasto-plastic, (c) fully developed plasticity.
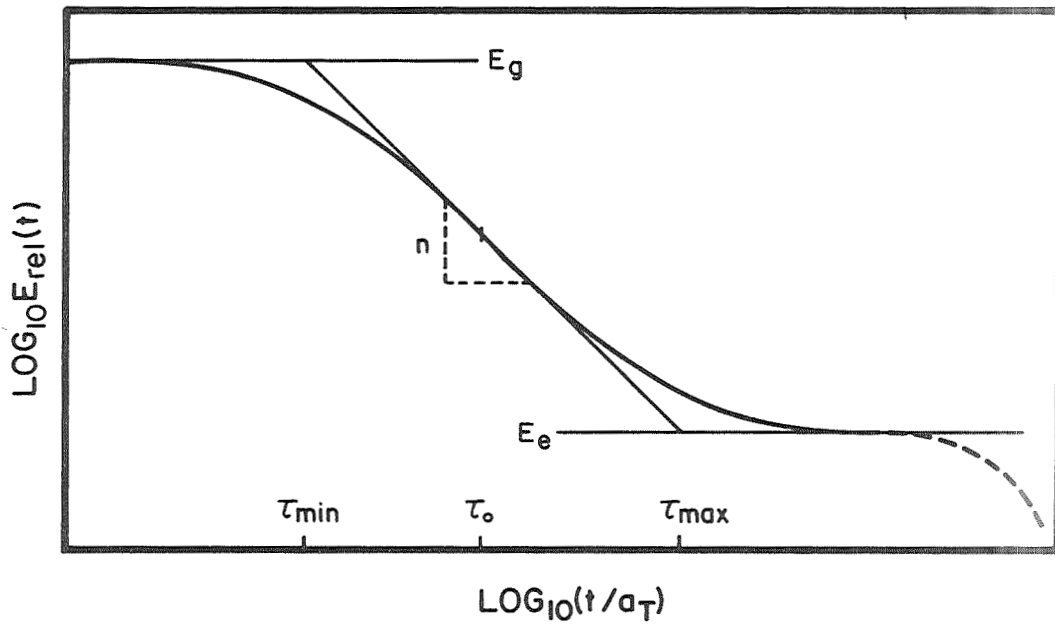
Figure 9. Modified power law approximation to the relaxation modulus. The actual behavior at long reduced time (dotted) is not reproduced by (102).
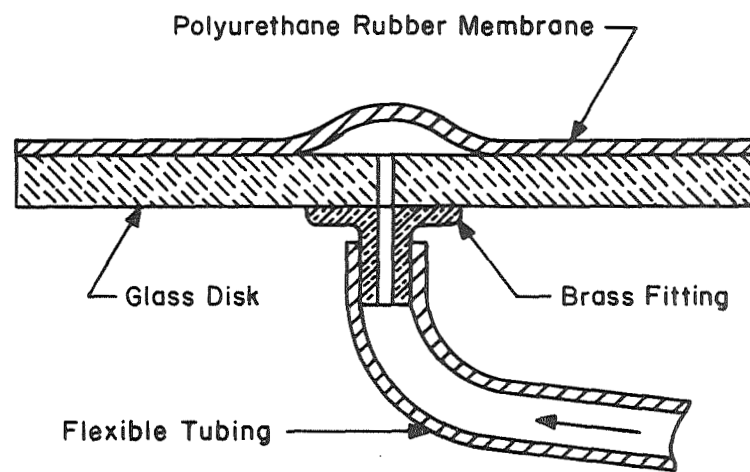
Figure 10. Sketch of pressurized blister specimen (Reference 32).
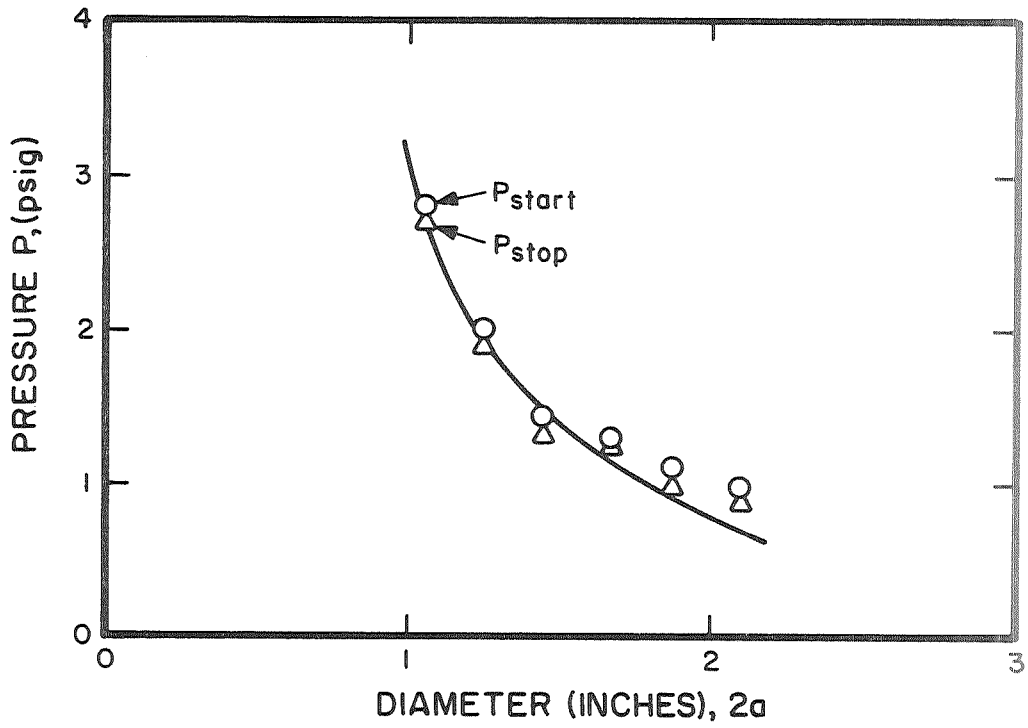
Figure 11. Typical pressure p versus diameter 2a data for the pressurized disk. E = 400 psi, h = 0.043 in., giving γ_a = 1.4 in.-lb/in^2 (Reference 32).
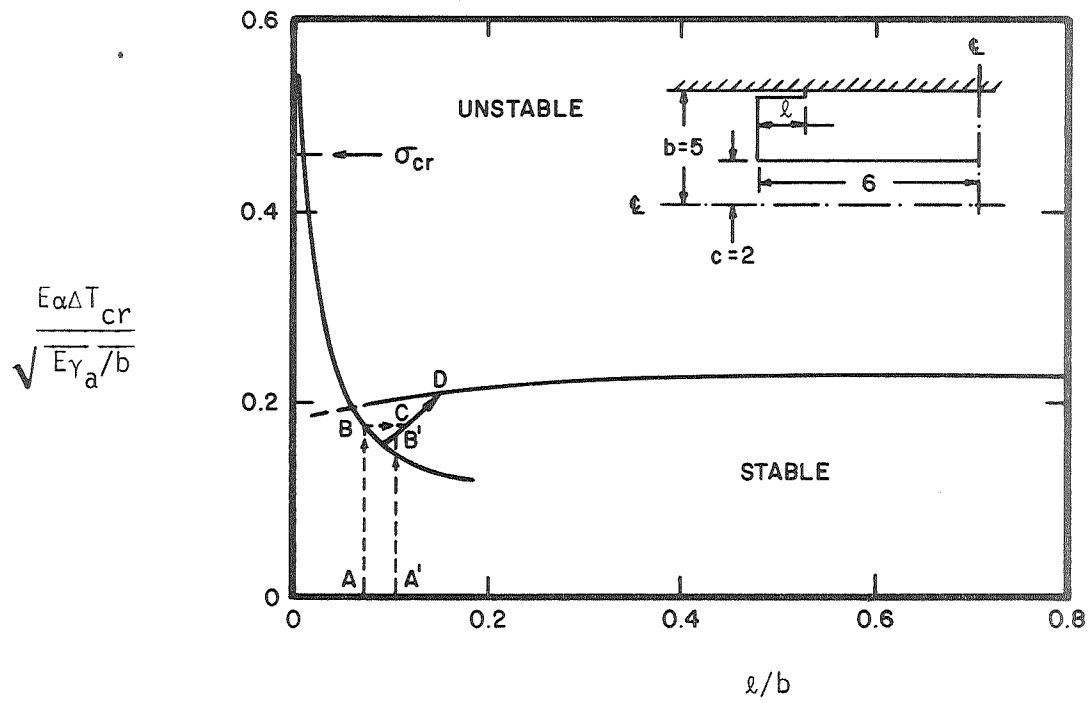
Figure 12. Predicted allowable temperature drop as a function
of crack length before debonding in a polyurethene
rubber tube in a quartz glass cylinder (Reference 7).
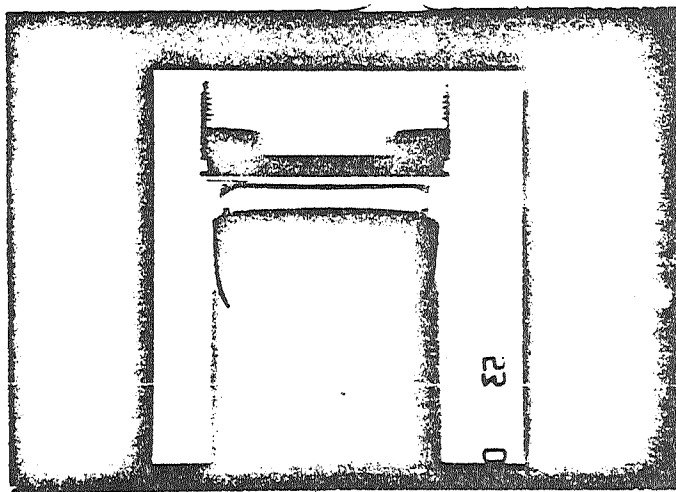
Figure 13. Photo of X-ray inspected solid rubber cylinder in a quartz glass tube subjected to temperature drop. Note cracks emanating from the end of the filler material at the interface with the glass.
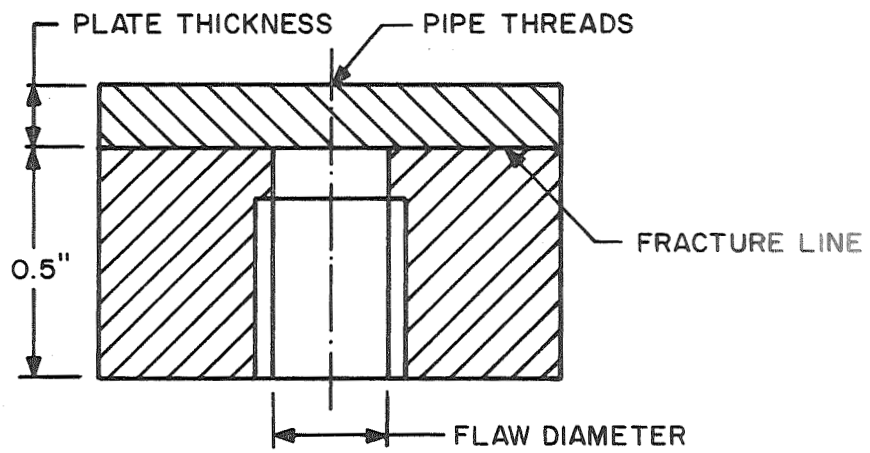
Figure 14a.   Explosively welded test sample configuration.
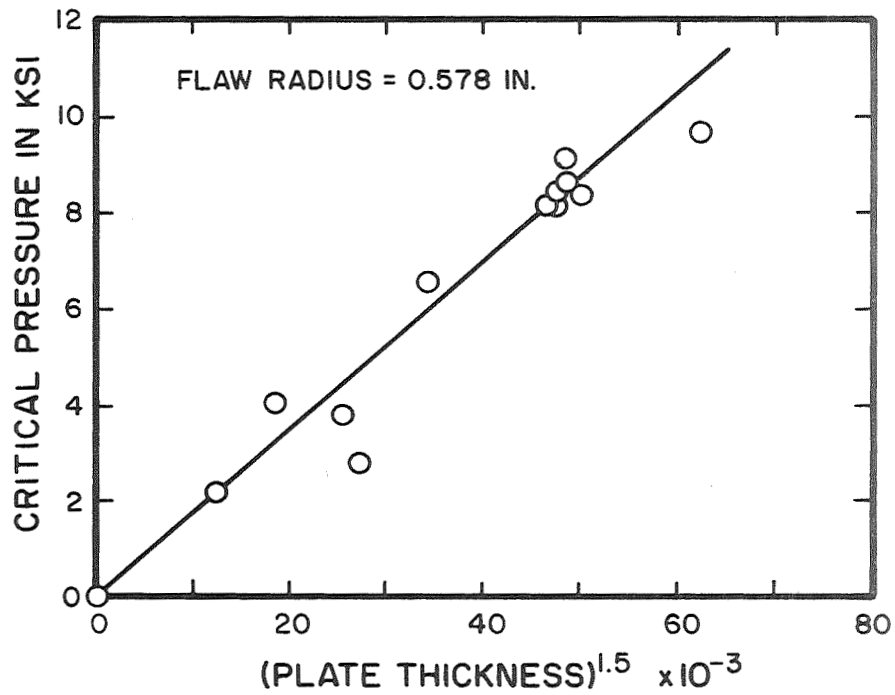
Figure 14b.   Preliminary test data demonstrating the relationship
between critical pressure and plate thickness which is
predicted by the theoretical model (Reference 35).

71
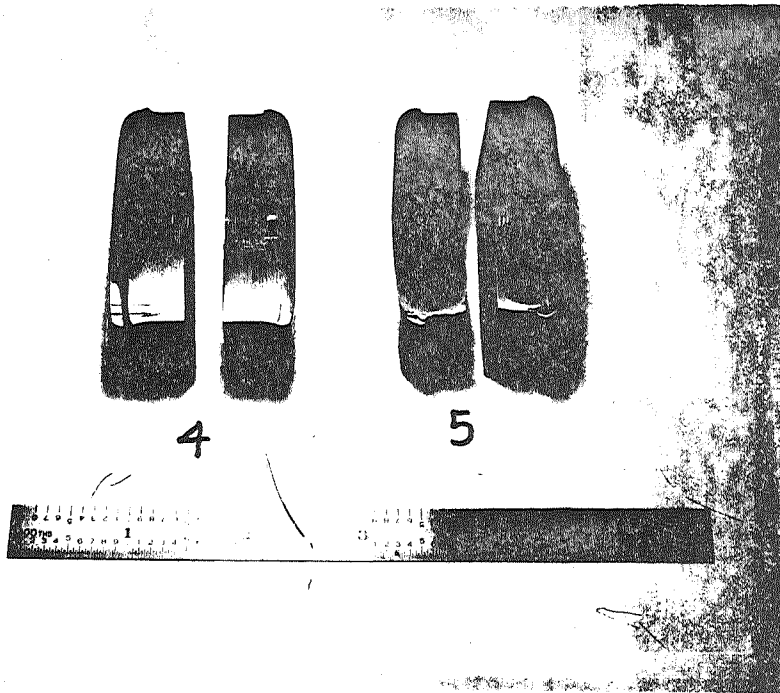
Figure 15. Section specimen of an explosively bonded steel
blister (Reference 35).
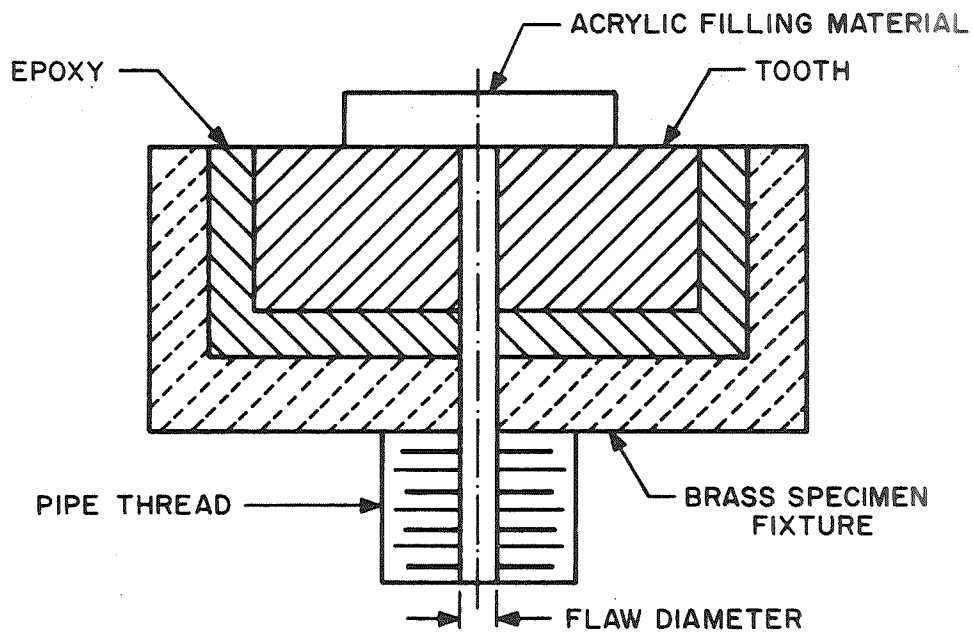
Figure 16.   Dental adhesive blister test specimen showing
commercially available dental filling material adhered
to elephant tusk surface preparation to standard
dental practice.

73
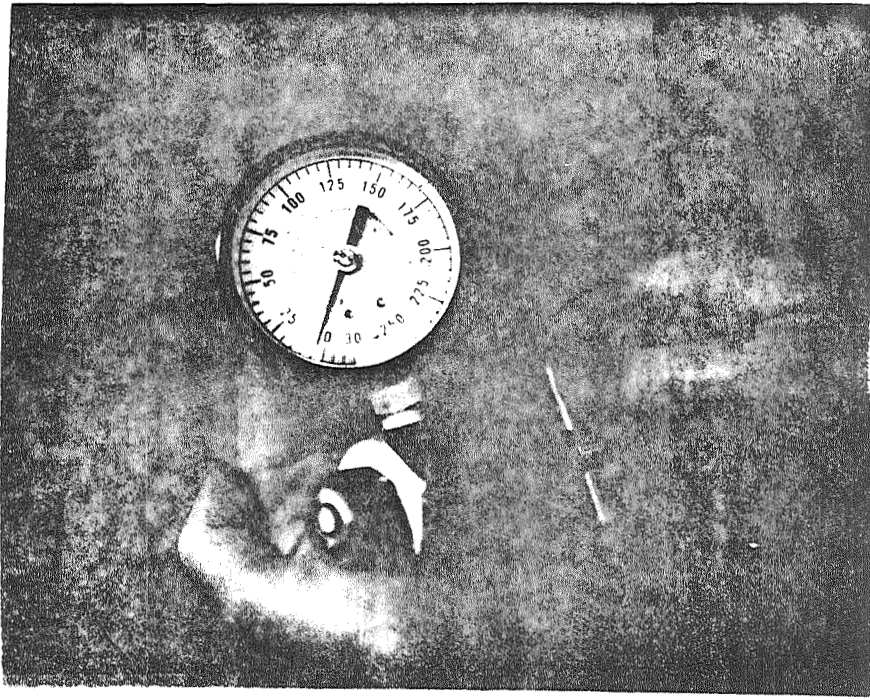
Figure 17a. Photograph of apparatus used to measure adhesive
energy of dental adhesives (Reference 36).
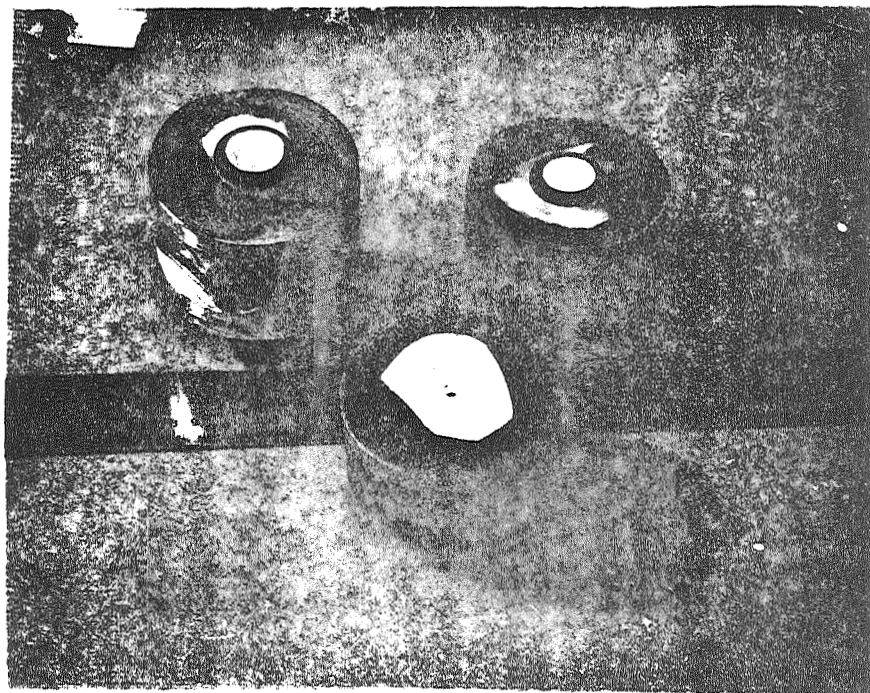
Figure 17b. Photograph of plugs used in adhesive energy apparatus
with bovine teeth, approximating analytical model of
Figure 4b (Reference 36).

74

Figure 18a.   Closeup of mature barnacle on PMMA after 3 months growth in salt water   (Reference 37).
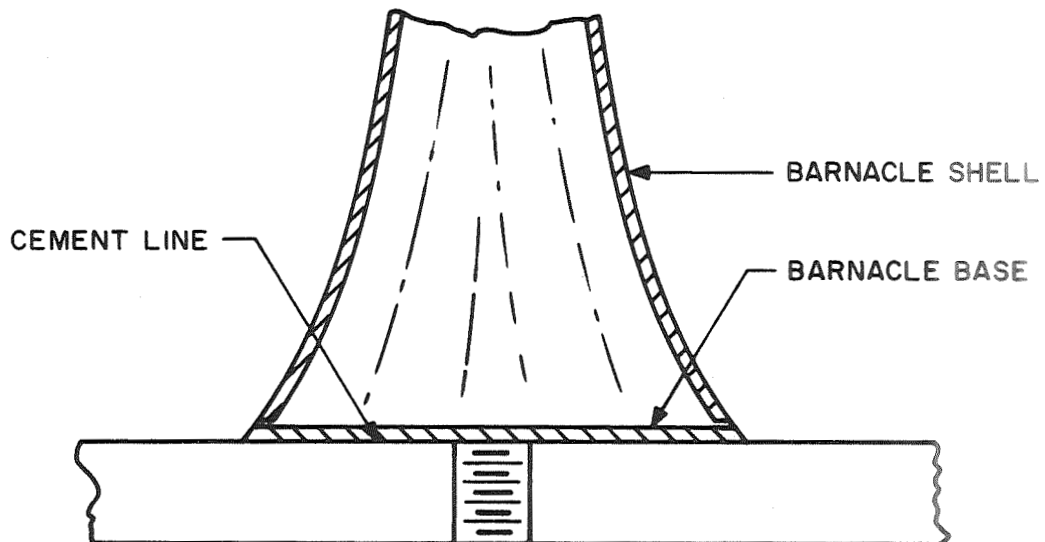

Figure 18b.   Experimental arrangement for determination of adhesive fracture energy of barnacle cement (Reference 37).
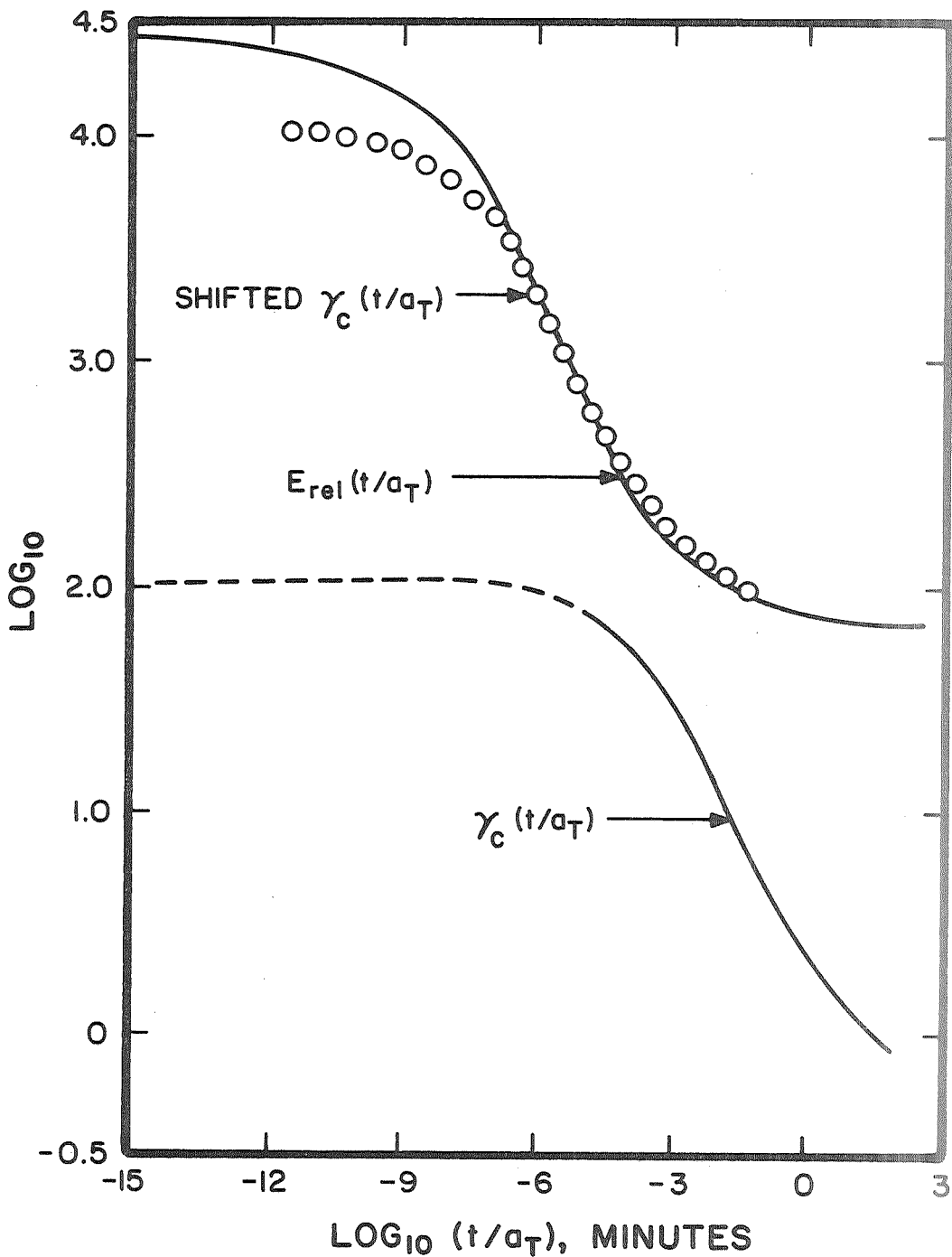
Figure 19. Log-log variation of a butadiene rubber relaxation modulus and cohesive fracture energy (Reference 26). A personal communication from S. J. Bennett reveals that he has established a tentative short time, low temperature limit value of approximately 100 in-lbs/in^2 for γ_c at a reduced time of $t/a_T = 10^{-9}$.
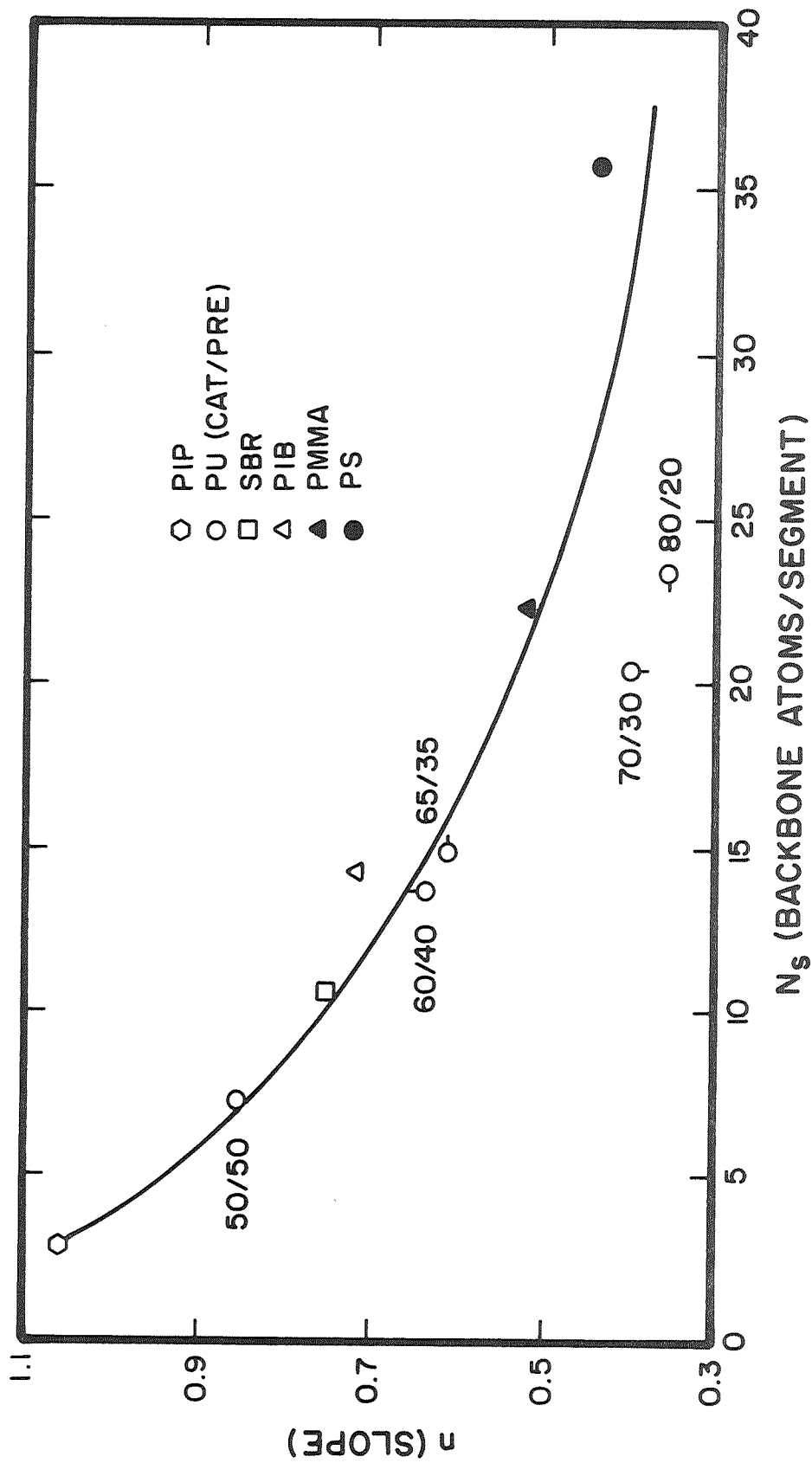
76

Figure 20. Plot of slope of the relaxation curve, n, against stiffness index, N_s, for several polymers. Circles are polyurethanes of nearly the same cross-link density, but varying catalyst to prepolymer ratios as indicated(71). Other polymers and associated references are ⬡ - polyisoprene(47,69), ☐ - SBR(69,70), △ - polyisobutylene(49,72), ◇ - polystyrene(49,72).

77